# Design, synthesis, characterization and biological studies of ruthenium and gold compounds with anticancer properties

Garza-Ortiz, A.

# CHAPTER 5

## Synthesis, Characterization and Cytotoxic Activity Studies of a New Family of Bis(arylimino)pyridine-Ru(II) Complexes. Further Look in the Tuning of the Cytotoxic Properties

**Abstract**

The coordination compounds $[RuLxCl_3]\cdot nH_2O$ (Lx=L1: 2,6-bis(2,4,6-trimethylphenyliminomethyl)pyridine or L2: 2,6-bis(2,6-diisopropylphenyliminomethyl)pyridine and in which n=0,1) have been used to study the reactivity and cytotoxic activity of a new family of $Ru^{2+}$ complexes. The synthesis, isolation and X-ray structures of the Ru(II)-bis(arylimino)pyridine complexes as chlorido-, 1,10-phenanthroline- (phen), 2,2'dipyridyl- (bpy), azpy-, 3mazpy-, tazpy-, and 2-picolinate-adducts (pic) are reported in an effort for further evaluation and modulation of the chemical reactivity and cytotoxicity. The complexes, incorporating bidentate ligands with different donor nature, are also designed to contain a monodentate chloride ligand, which would be easily substituted. Elemental analysis and several spectroscopic techniques (IR, UV-vis, $^1$H NMR and ESI-MS) have been used in the characterization of these Ru(II) compounds. A complete assignment of the $^1$H NMR resonance spectra was achieved thorugh the integration values, multiplicity of resonance peaks, deshielding effects and two-dimensional techniques.

The *in vitro* evaluation of the cytotoxic properties of these new Ru(II) complexes in comparison with the parent, starting Ru(III)-compounds ($IC_{50}$ values = 4 ~ 17 μM) led to significant improvement in cytotoxicity ($IC_{50}$ values =0.4 ~ 10 μM) for a broad range of cancer cell-lines tested. Some of them show even better cytotoxic effects than cisplatin. The most active family of compounds, in terms of cytotoxicity, is the one containing the 2,6-bis(2,6-diisopropylphenyliminomethyl)pyridine tridentate ligand. These studies are expected to be of help in the understanding and establishment of useful structure-activity relationships for this family of compounds.

5

*While you are experimenting, do not remain content with the surface of things. Do not become a mere recorder of facts but try to penetrate the mystery of their origins*
***Isabel Allende, Writer (1942-)***

## 5.1 Introduction

The field of coordination chemistry of ruthenium has grown exponentially in the last decades due to the multiple applications in fields like catalysis, photochemistry and photophysics, supramolecular and bioinorganic chemistry [1, 2]. In this last field important biological activity for Ru complexes, as anticancer agents, has been widely demonstrated. It is clear that the interest in the chemistry of ruthenium compounds is primarily due to the versatile electron-transfer properties exhibited by complexes of this metal, as variation in the coordination environment around ruthenium, can be designed to modulate the redox properties of its complexes and as a consequence, the biological properties as well. Also of importance is the thermodynamic and kinetic stability of Ru(III) and Ru(II) compounds as ligand exchange kinetics are directly affected.

As has been repeatedly described in the literature, a versatile reactivity is exhibited by Ru complexes, most of which originates from the relative weakness of one or more metal-ligand bond(s). For instance, ruthenium coordination compounds having a single Ru-Cl bond often give rise to interesting chemistry, involving dissociation of this Ru-Cl bond [3-6].

Interestingly, Ru compounds such as *mer*-[Ru(III)(tpy)$Cl_3$] [7, 8]; [Ru(III)$(NH_3)_3Cl_3$] [9]; $\alpha$-, $\beta$- and $\gamma$-[Ru(II)$(azpy)_2Cl_2$] [10-12]; several Ru(II) half-sandwich complexes [13-16]; KP1019(Ru(III)) and its derivatives [17-19] and [Ru(IV)$(H_2cdta)Cl_2$] ($H_4$cdta: 1,2-cyclohexanediaminotetraacetic acid) [20-22], have been found to be from highly to moderately cytotoxic in cell cultures, while other Ru compounds such as [Ru(II)$(dmso)_4Cl_2$] [23]; NAMI-A(Ru(III)) [19, 24]; and the arene PTA Ruthenium(II) (RAPTA) complexes (pta:1,3,5-triaza-7-phosphatricyclo[3.3.1.1]decane) [25-27] are –moderate to poorly- active *in vitro* antiproliferative agents, but highly selective and active as antimetastatic *in vivo* compounds [23].

Ru(II)-pyridine bidentate *tris*-chelate compounds show DNA-intercalation properties and in particular, KP1019 and its derivatives were probed to bind to the Fe(III) active sites in the proteins lactoferrin and transferrin [9, 18, 28-34]. Lactoferrin and transferrin are considered responsible for the delivery of Ru(III) complexes into the cancer cells, where it is believed that an *in vivo* reduction to the Ru(II) form takes place, which is kinetically more active than Ru(III).

In view of the above facts, and in order to obtain more evidence that could eventually support the “activation by reduction” hypothesis [28] that has been propose as responsible for the biological activity of some ruthenium compounds, a number of novel Ru(II) complexes has now been synthesized, characterized and biologically tested.

In the previous chapter the synthesis, isolation, characterization and cytotoxic activity determination of a family of mononuclear Ru(III) compounds were fully described. Continuing the search of potential anticancer drug candidates in ruthenium complexes, a closely related family of mononuclear Ru(II)-bis(arylimino)pyridine compounds is described in this chapter.

The ruthenium polypyridyl chemistry has been developed at high speed due mainly to the extensive and detailed synthetic chemistry. No other metallic compounds, with the possible exception of ferrocene, show similar stability and flexibility [35]. Since polypyridine ligands are known to stabilize ruthenium in its +2 oxidation state, the bidentate ligands, 2,2’-dipyridyl (bpy) and 1,10-phenantroline (phen) have been successfully coordinated to [RuLx$Cl_3$]·n$H_2O$ (Lx=L1: 2,6-bis(2,4,6-trimethylphenyliminomethyl)pyridine or L2: 2,6-bis(2,6-diisopropylphenyliminomethyl) pyridine and n=0,1). The complexes incorporating these bidentate ligands, and isolated as their perchlorate salts, are also designed to contain a monodentate chloride ligand, which could be substituted later.

Even more and in continuation with the interest on the chemical and biological properties of Ru(II) compounds with 2-(arylazo)pyridine ligands, the compounds [RuLx$Cl_3$]·n$H_2O$ (Lx=L1: 2,6-bis(2,4,6-trimethylphenyliminomethyl)pyridine or L2: 2,6-bis(2,6-diisopropylphenyliminomethyl) pyridine and n=0,1) were reacted in presence of the bidentate (Npyridine, Nazo) ligands: azpy, 3mazpy and tazpy and the mononuclear products isolated as their perchlorate salts. This set of ligands was selected mainly due to the remarkably *in vitro* antitumour activity of $\alpha$-[Ru(II)$(azpy)_2Cl_2$]. The higher cytotoxic activity of $\alpha$-[Ru(II)$(azpy)_2Cl_2$] in comparison with the cytotoxic activity developed by *cis*-[Ru(II)$(bpy)_2Cl_2$] has been explained as a result of higher flexibility of the azpy ligand which provides an easier substitution of the chloride ligand which is completing the octahedral geometry [12, 36]. The ligands selected for this study are closely related arylazopyridines, containing electron-donating groups, either in the pyridyl moiety, or in the

phenyl moiety in an attempt to tune both, the best stability and biological activity of the new Ru(II) compounds.

Finally, a fine tuning of the chemical and biological properties of the family of Ru(II) compounds discussed in this research project, could be reached by alteration of the coordination sphere around the metal centre and that is the reason that the anionic bidentate (N, O) chelating ligand, 2-picolinic acid (pic-H) was used in order to synthesize new Ru(II)-bis(arylimino)pyridine complexes. The carboxylate oxygen is considered as a hard donor and known to stabilize lower oxidation states of ruthenium [37]. All these attempts for tuning the structural and chemical properties of the Ru(II) compounds are intended to fulfilling different requirements for biological activity.

In the following sections, synthesis, isolation, characterization by several spectroscopic techniques and X-ray structures of some Ru(II)-bis(arylimino)pyridine complexes, as chlorido-, 1,10-phenanthroline, 2,2'-dipyridyl-, azpy-, 3mazpy-, tazpy-, and 2-picolinate-adducts, will be discussed. Finally, *in vitro* evaluation of the cytotoxic properties of these new Ru(II) complexes will be analyzed in view of developing useful structure-activity relationships.

## 5.2 Experimental section

### 5.2.1 Methods and instrumental techniques

Chemicals and solvents (analytical reagent grade) were purchased from Acros, Nova-Biochem and Biosolve and used without further purification treatments unless otherwise stated.

**A. X-ray Crystallography.** Good quality crystals for X-ray diffraction studies were obtained for RuL2-bpy, RuL2-phen and RuL1-pic. All reflections intensities were measured at 150(2) K, using a Nonius KappaCCD diffractometer (fine-focus sealed tube) equipped with graphite-monochromated Mo K$\alpha$ radiation ($\lambda$ = 0.71073 Å) under the program *COLLECT* [38]. The program *PEAKREF* [39] was used to determine the cell dimensions. The sets of data were integrated using the program *EVALCCD* [40]. The structure of RuL1-pic, RuL2-phen and RuL2-bpy were solved with the program *DIRDIF99* [41]. All the structures were refined on $F^2$ with *SHELXL97* [42]. Multi-scan semi-empirical absorption corrections were applied to the sets of data using *SADABS* [43]. For RuL1-pic, 6399 reflections were unique ($R_{int}$ = 0.028), of which 5366 were observed ($\theta_{max}$ = 27.4°) with the criterion of $I > 2\sigma(I)$; for RuL2-phen, 11150 reflections were unique ($R_{int}$ = 0.036), of which 9188 were observed ($\theta_{max}$ = 27.5°) with the criterion of $I > 2\sigma(I)$; and for RuL2-bpy, 10557 reflections were unique ($R_{int}$ = 0.036), of which 8789 were observed ($\theta_{max}$ = 27.5°) with criterion of $I > 2\sigma(I)$. The *PLATON* software [44] was used for molecular graphics, structure checking and calculations. The H atoms were placed at calculated positions (except as specified) with isotropic displacement parameters having values 1.2 or 1.5 times $U_{eq}$ of the attached atom. Crystallographic data for RuL2-bpy, RuL2-phen and RuL1-pic are listed in tables 5.2 and 5.3.

**B. NMR Spectroscopy.** $^1$H NMR experiments were recorded on a Bruker 300 DPX spectrometer using 5-mm NMR tubes. All spectra were recorded at 294 K, unless otherwise indicated. The temperature was kept constant using a variable temperature unit. The software XWIN-NMR and XWIN-PLOT were used for edition of the NMR spectra. Tetramethylsilane (TMS) or the deuterated solvent residual peaks were used for calibration. In addition, 2D $^1$H COSY spectra were recorded to confirm the proton assignments from 1D measurements.

**C. C,H,N Analysis.** Elemental analyses were performed with a Perkin Elmer series II CHNS/O 2400 Analyzer.

**D. Mass Spectroscopy.** Electrospray mass spectra were recorded on a Finnigan TSQ-quantum instrument using an electrospray ionization technique (ESI-MS). The eluent used was a mixture acetonitrile:water 80:20.

**E. Other methods.** The UV-Visible (UV-Vis) spectra were recorded using a Varian CARY 50 UV/VIS spectrophotometer operating at RT. The electronic spectra were recorded in freshly

prepared solutions of each compound. The IR spectra obtained for the products mentioned in this work, in the 4000-300 $cm^{-1}$ range, were recorded as solids with a Perkin Elmer FT-IR Paragon 1000 spectrophotometer with a single-reflection diamond ATR P/N 10500.

**F. Cytotoxicity and $IC_{50}$ determination.** The *in vitro* cytotoxicity test of compounds L1, and RuL1 were performed using the SRB test [45] for estimation of cell viability. The human cell lines MCF-7 (breast cancer), EVSA-T (breast cancer), WIDR (colon cancer), IGROV (ovarian cancer), M19-MEL (melanoma cancer), A498 (renal cancer) and H226 (non-small cell lung cancer) were used. Cell lines WIDR, M19 MEL, A498, IGROV and H226 belong to the currently used anticancer screening panel of the National Cancer Institute, USA [46]. The MCF-7 cell line is an oestrogen receptor $(ER)^+$/ progesterone receptor $(PgR)^+$ and the cell line EVSA-T is $(ER)^-/(PgR)^-$. Prior to the experiments a mycoplasma test was carried out on all cell lines and found to be negative. All the cell lines were maintained in a continuous logarithmic culture in RPMI 1640 (Invitrogen, Paisley Scotland) medium with Hepes and phenol red. The medium was supplemented with 10% foetal calf serum (Invitrogen, Paisley Scotland), penicillin 100 IU/mL (Sigma, USA) and streptomycin 100μg/mL (Sigma, USA). The cells were mildly trypsinized for passage and for use in the experiments. For the cell-growth assay, cells (1500-2000 cells/150 μl of complete medium/well) were pre-cultured in 96 multi-well plates (falcon 3072, BD) for 48 h at 37 ºC in a 5% $CO_2$-containing incubator and subsequently treated with the tested compounds for 5 days. The stock solutions of the compounds were prepared in the corresponding medium. A three-fold dilution sequence of ten steps was made in full medium, starting with the 250000 ng/mL stock solution. Every dilution was used in quadruplicate by adding 50 μL to a column of wells. The result in the highest concentration of 62500 ng/mL is present in column 12. Column 2 was used for the blank and column 1 was completed with medium to diminish interfering evaporation. After a 120 h incubation time, the surviving cells in cultures, treated with the compounds were detected, using the sulforhodamine B (SRB, sigma,USA) test [45]. After the incubation time cells were fixed with 10% of trichloroacetic acid (sigma, USA) in PBS (Emmer-Compascuum, NL). After three washing cycles with tap water, the cells were stained for at least 15 minutes with 0.4% SRB dissolved in 1% of acetic acid (Baker BV, NL). After staining, the cells were washed with 1% acetic acid to remove the unbound stain. The plates were air-dried and the bound stain was dissolved in 150 μL of 10mM Tris-buffer (tris(hydroxymethyl)aminomethane). The absorbance was read at 540 nm using an automated microplate reader (Labsystems Multiskan MS). Data were used for construction of concentration-response curves and determination of the $ID_{50}$ values was graphically done by use of Deltasoft 3 software. The variability of the *in vitro* cytotoxicity test depends on the cell line used and the serum applied. With the same batch of cell lines and the same batch of serum the inter-experimental CV (coefficient of variation) is 1-11%, depending on the cell line and the intra-experimental CV is 2-4%. These values may be higher when using other batches of cell lines and/or serum [47].

### 5.2.2 Synthetic procedures

Chemicals and solvents (analytical reagent grade) were purchased from Acros, Nova-Biochem and Biosolve and used without further purification treatments unless otherwise stated. The synthetic procedures for RuL1, RuL2, azpy, 3mazpy and tazpy have been fully described in chapters 2 and 4. 2-picolinic acid was purchased from Fluka while 1,10-phenantroline and 2,2'-dipyridyl were purchased from Sigma-Aldrich. All other reagents were of high purity and used as purchased without any further purification. Ruthenium trichloride hydrate was a generous gift from Johnson Matthey, UK. All synthesized compounds are reasonably thermally stable and air-stable, both in the solid state and in solution. For caution's sake, however, their preparation and manipulation in solution were carried out under an inert atmosphere (Ar).

**A. Synthesis of chlorido(2-(phenylazo)pyridine)(2,6-bis(2,4,6-trimethylphenyliminomethyl) pyridine)ruthenium(II) perchlorate hydrate, RuL1-azpy.** This compound was synthesized by a procedure described as follows: RuL1 (20 mg, 0.034 mmol, 1 Eq) and azpy (9.62 mg, 0.0525 mmol, 1.5 Eq) were gently refluxed for 1h in 3 mL of a mixture ethanol/water (70:30) containing LiCl (20 mg, 0.47 mmol) and triethylamine (0.006 mL). At the end of the reaction time, the hot

reaction mixture was filtered to remove any insoluble material. The volume of the filtrate was reduced one third by rotary evaporation and cooled at RT. 1.0 mL of an aqueous saturated $NaClO_4$ solution was added. After some days the formed solid was collected by filtration, washed with plenty of cold water, cold chloroform and dried with dry diethyl ether. Yield: 69 % (0.024 mmol, 19.03 mg). Elemental analysis for $RuC_{36}H_{36}N_6Cl_2O_4 \cdot H_2O$: Calculated (%): C, 53.60; N, 10.42 and H, 4.75. Found (%): C, 53.35; N, 10.32 and H, 4.90. ESI-MS: m/z=689, $[RuL1\text{-}azpy - H_2O - ClO_4]^+$, 100%, where calculated m/z=689.25. IR: 3200-2900, 1599, 1500-1450, 1295, 1242, 1195-1140, 1090, 962, 852, 806-744, 622, 590-544, 500-460, 388 and 318 $cm^{-1}$. UV-Vis in acetonitrile ($\lambda_{max}(\log\varepsilon_M)$): 353(4.25) and 557(4.00). $^1H$ NMR (400 MHz, deuterated acetonitrile, 294 K, s=singlet, d=doublet, t=triplet and m=multiplet): $\delta$=9.63(d, 1H), 8.31(d, 2H), 8.26(s, 2H), 8.23(d, 1H), 8.18(t, 1H), 7.98(t, 1H), 7.62(t, 1H), 7.56(t, 1H), 7.38(m, 4H), 6.56(s, 2H), 6.48(s, 2H), 2.19(s, 6H), 2.03(s, 6H) and 1.11 ppm (t, 6H).

**B. Synthesis of chlorido(2,2'-dipyridyl)(2,6-bis(2,4,6-trimethylphenyliminomethyl)pyridine) ruthenium(II) perchlorate hydrate, RuL1-bpy.** For the synthesis of this compound the previously described synthetic procedure was applied. RuL1 (50 mg, 0.084 mmol, 1 Eq) and bpy (19.69 mg, 0.1260 mmol, 1.5 Eq) were gently refluxed for 1h in 7.5 mL of a mixture ethanol/water (70:30) containing LiCl (50 mg, 1.18 mmol) and triethylamine (0.015 mL). At the end of the reaction time, the hot reaction mixture is filtered to remove any insoluble material. The volume of the filtrate is reduced one third by rotary evaporation and cooled at RT. 2.5 mL of an aqueous saturated $NaClO_4$ solution was added. After some days the formed solid was collected by filtration, washed with plenty of cold water, cold chloroform and dried with dry diethyl ether. Yield: 72 % (0.061 mmol, 47.4 mg). Elemental analysis for $RuC_{35}H_{35}N_5Cl_2O_4 \cdot H_2O$: Calculated (%): C, 53.92; N, 8.98 and H, 4.78. Found (%): C, 54.02; N, 9.11 and H, 4.69. ESI-MS: m/z=661.78, $[RuL1\text{-}bpy - H_2O - ClO_4]^+$, 100%, where calculated m/z=662.22. IR: 3200-2900, 1600, 1505-1418, 1393, 1295, 1268, 1195-1139, 1090, 856, 794-784, 762-728, 622, 594, 384 and 324 $cm^{-1}$. UV-Vis in acetonitrile ($\lambda_{max}(\log\varepsilon_M)$): 241(4.62), 293(4.43) and 491(4.07). $^1H$ NMR (300 MHz, deuterated acetonitrile, 294 K, s=singlet, d=doublet, t=triplet and m=multiplet): $\delta$=9.91(d, 1H), 8.67(s, 2H), 8.46(d, 2H), 8.22(m, 4H), 7.99(dd, 2H), 7.76(t, 1H), 7.42(t, 1H), 6.60(s, 2H), 6.44(s, 2H), 2.81(s, 6H) 2.31(s, 6H) and 1.07(s, 6H).

**C. Synthesis of chlorido(2-(phenylazo)-3-methypyridine)(2,6-bis(2,4,6-trimethylphenylimino methyl)pyridine)ruthenium(II) perchlorate, RuL1-3mazpy.** For the synthesis of this compound the previously described synthetic procedure was applied with the following reagents. RuL1 (50 mg, 0.084 mmol, 1 Eq), 3-mazpy (24.86 mg, 0.1260 mmol, 1.5 Eq), LiCl (50 mg, 1.18 mmol) and triethylamine (0.015 mL). Yield: 33 % (0.0278 mmol, 22.28 mg). Elemental analysis for $RuC_{37}H_{38}N_6Cl_2O_4$: Calculated (%): C, 55.36; N, 10.47 and H, 4.77. Found (%): C, 55.57; N, 10.66 and H, 4.81. ESI-MS: m/z=702.76, $[RuL1\text{-}3mazpy - ClO_4]^+$, 100%, where calculated m/z=703.27. IR: 3200-2900, 1650-1558, 1472-1436, 1381, 1317, 1244, 1196, 1082, 850, 770, 742, 690, 622, 460, 376 and 326 $cm^{-1}$. UV-Vis in acetonitrile ($\lambda_{max}(\log\varepsilon_M)$): 354(4.21) and 557(3.95). $^1H$ NMR (300 MHz, deuterated acetonitrile, 294 K, s=singlet, d=doublet, t=triplet and m=multiplet): $\delta$=9.53(d, 1H), 8.67(s, 2H), 8.60(d, 2H), 8.39(t, 1H), 7.92(s, 1H), 7.72(dd, 1H), 7.62(m, 3H), 7.46(t, 2H), 6.60(s, 2H), 6.56(s, 2H), 2.79(s, 6H) 2.58(s, 3H), 2.20(s, 6H) and 1.24 ppm (s, 6H).

**D. Synthesis of chlorido(1,10-phenanthroline)(2,6-bis(2,4,6-trimethylphenylimino methyl)pyridine)ruthenium(II) perchlorate, RuL1-phen.** The same synthetic procedure as for C: RuL1 (50 mg, 0.084 mmol, 1 Eq), phen (22.71 mg, 0.1260 mmol, 1.5 Eq), LiCl (50 mg, 1.18 mmol) and triethylamine (0.015 mL). Yield: 56% (0.0471 mmol, 36.98 mg). Elemental analysis for $RuC_{37}H_{35}N_5Cl_2O_4$: Calculated (%): C, 56.56; N, 8.91 and H, 4.49. Found (%): C, 56.33; N, 8.81 and H, 4.50. ESI-MS: m/z=685.73, $[RuL1\text{-}phen - ClO_4]^+$, 100%, where calculated m/z=686.24. IR: 3200-2900, 1599-1506, 1472-1382, 1194, 1140, 1080, 842, 788-738, 720, 622, 524-470, 390, 382, and 328 $cm^{-1}$. UV-Vis in acetonitrile ($\lambda_{max}(\log\varepsilon_M)$): 265(4.53), 360(3.75) and 491(4.03). $^1H$ NMR (300 MHz, deuterated acetonitrile, 294 K, s=singlet, d=doublet, t=triplet and m=multiplet): $\delta$=10.13(d, 1H), 8.68(s, 2H), 8.60(m, 3H), 8.50(d, 1H), 8.19(t, 1H), 8.10(m, 3H), 7.76(dd, 1H), 6.47(s, 2H), 6.12(s, 2H), 2.79(s, 6H), 2.34(s, 6H) and 0.85 ppm (s, 6H).

**E. Synthesis of chlorido(2-picolinate)(2,6-bis(2,4,6-trimethylphenylimino methyl)pyridine)ruthenium(II), RuL1-pic.** RuL1-pic was synthesized with a procedure based in a previously reported synthetic procedure by Chatterjee *et al.* [48] where $[Ru(II)(tpy)(pic)(H_2O]ClO_4$ was successfully prepared. RuL1 (50 mg, 0.084 mmol, 1 Eq) and 2-picolinic acid (10.34 mg, 0.084 mmol, 1.0 Eq) were gently refluxed in 4 mL of a mixture ethanol/water (75:25) containing LiCl (22.26 mg, 1.03 mmol) and triethylamine (0.02 mL). After a 3 h reflux, the resultant mixture is filtered while hot to remove any insoluble material. The filtrate is cooled down and the volume of the filtrate is reduced by rotary evaporation. A dark precipitate is obtained and collected in a Sartorius filter. It is washed with chilled HCl, 3 M followed by acetone and dried with dry diethyl ether. Yield: 73 % (0.0612 mmol, 38.60 mg). X-ray quality crystals were obtained by slow evaporation of a concentrated solution of RuL1-pic in acetonitrile. Elemental analysis for $RuC_{31}H_{31}N_4ClO_2$: Calculated (%): C, 59.28; N, 8.92 and H, 4.97. Found (%): C, 58.85; N, 8.59 and H, 4.75. ESI-MS: m/z=651.80, $[RuL1\text{-}pic - Cl + H_2O + CH_3CN]^+$, where calculated m/z=651.75; m/z=628.12, $[RuL1\text{-}pic]^+$, 100%, where calculated m/z=628.13. IR: 3200-2900, 1635, 1602, 1472-1436, 1381, 1326, 1284, 1196, 848, 782-747, 692, 601-590, 334 and 324 $cm^{-1}$. UV-Vis in acetonitrile ($\lambda_{max}(\log\varepsilon_M)$): 232(4.85), 302(4.09) and 500(4.00). $^1H$ NMR (300 MHz, deuterated acetonitrile, 294 K, s=singlet, d=doublet, t=triplet and m=multiplet): $\delta$=9.85(d, 1H), 8.62(s, 2H), 8.20(d, 2H), 8.12(t, 1H), 7.76(t, 1H), 7.45(m, 2H), 6.60(s, 2H), 6.54(s, 2H), 2.86(s, 6H), 2.20(s, 6H) and 1.185 ppm (s, 6H).

**F. Synthesis of chlorido(2-(tolylazo)pyridine)(2,6-bis(2,4,6-trimethylphenyliminomethyl) pyridine)ruthenium(II) perchlorate, RuL1-tazpy.** For this compound an identical synthetic procedure to RuL1-3mazpy was applied. RuL1(50 mg, 0.084 mmol, 1 Eq), tazpy (24.86 mg, 0.1260 mmol, 1.5 Eq), LiCl (50 mg, 1.18 mmol) and triethylamine (0.015 mL). Yield: 93 % (0.785 mmol, 63.03 mg). Elemental analysis for $RuC_{37}H_{38}N_6Cl_2O_4$: Calculated (%): C, 55.36; N, 10.47 and H, 4.77. Found (%): C, 55.10; N, 10.47 and H, 4.55. ESI-MS: m/z=702.76, $[RuL1\text{-}tazpy - ClO_4]^+$, 100%, where calculated m/z=703.23. IR: 3200-2900, 1599, 1520, 1480-1452, 1379, 1309, 1242, 1081, 960, 852, 807-717, 676, 622, 388 and 328 $cm^{-1}$. UV-Vis in acetonitrile ($\lambda_{max}(\log\varepsilon_M)$): 321(4.21), 366(4.15) and 556(3.99). $^1H$ NMR (300 MHz, deuterated acetonitrile, 294 K, s=singlet, d=doublet, t=triplet and m=multiplet): $\delta$=9.87(d, 1H), 8.61(s, 2H), 8.55(d, 2H), 8.35(m, 2H), 8.12(t, 1H), 7.84(t, 1H), 7.57(d, 1H), 7.41(m, 2H), 7.24(t, 1H), 6.59(broad s, 4H), 2.79(s, 6H), 2.27(s, 6H), 1.63(s, 3H) and 1.42 ppm (s, 6H).

The following compounds were synthesized through the procedures just described so in the coming lines only the chemical and physical analytical information of each compound will be described.

**G. Synthesis of chlorido(2-(phenylazo)pyridine)(2,6-bis(2,6-diisopropylphenyliminomethyl) pyridine)ruthenium(II) perchlorate, RuL2-azpy.** RuL2 (50 mg, 0.0756 mmol, 1 Eq), azpy (20.78 mg, 0.1134 mmol, 1.5 Eq), LiCl (50 mg, 1.18 mmol) and triethylamine (0.015 mL). Yield: 74 % (0.0559 mmol, 48.79 mg). Elemental analysis for $RuC_{42}H_{48}N_6Cl_2O_4$: Calculated (%): C, 57.79; N, 9.63 and H, 5.54. Found (%): C, 57.24; N, 9.51 and H, 5.77. ESI-MS: m/z=772.83, $[RuL2\text{-}azpy - ClO_4]^+$, 100%, where calculated m/z=773.41. IR: 3200-2800, 1615-1580, 1520, 1460-1365, 1296, 1246, 1090, 959, 805-744, 622, 590, 482, 410, 322, and 310 $cm^{-1}$. UV-Vis in acetonitrile ($\lambda_{max}(\log\varepsilon_M)$): 231(4.63), 344(4.21) and 566(3.98). $^1H$ NMR (400 MHz, deuterated acetonitrile, 294 K, s=singlet, d=doublet, t=triplet and m=multiplet): $\delta$=9.51(d, 1H), 8.79(s, 2H), 8.76(d, 2H), 8.53(m, 2H), 8.17(t, 1H), 7.85(m, 3H), 7.70(t, 1H), 7.53(t, 2H), 7.08(m, 4H), 6.87(d, 2H), 3.84(m, 2H), 1.70(m, 2H), 1.15(d, 6H), 0.95(d, 6H), 0.64(d, 6H) and 0.42 ppm (d, 6H).

**H. Synthesis of chlorido(2,2'-dipyridyl)(2,6-bis(2,6-diisopropylphenyliminomethyl)pyridine) ruthenium(II) perchlorate, RuL2-bpy.** RuL2(50 mg, 0.0756 mmol, 1 Eq), bpy (17.71 mg, 0.1134 mmol, 1.5 Eq), LiCl (50 mg, 1.18 mmol) and triethylamine (0.015 mL). X-ray quality crystals were obtained by slow evaporation of a concentrated solution of RuL2-bpy in acetonitrile. Yield: 81 % (0.062 mmol, 52.07 mg). Elemental analysis for $RuC_{41}H_{47}N_5Cl_2O_4$: Calculated (%): C, 58.22; N, 8.28 and H, 5.60. Found (%): C, 58.81; N, 8.50 and H, 5.52. ESI-MS: m/z=745.87, $[RuL2\text{-}bpy - ClO_4]^+$, 100%, where calculated m/z=746.38. IR: 3200-2800, 1604, 1506-1420, 1386, 1364, 1273,

1089, 806, 769-732, 622, 588, 418-408 and 316 $cm^{-1}$. UV-Vis in acetonitrile ($\lambda_{max}(\log\varepsilon_M)$): 237(4.55), 292(4.41) and 492(3.99). $^1H$ NMR (300 MHz, deuterated acetonitrile, 294 K, s=singlet, d=doublet, t=triplet and m=multiplet): $\delta$=9.94(d, 1H), 8.72(s, 2H), 8.56(d, 2H), 8.35 (m, 3H), 8.22(t, 1H), 8.04(m, 2H), 7.86(t, 1H), 7.57(t, 1H), 7.03(m, 4H), 6.86(d, 2H), 4.16(m, 2H), 1.64(m, 2H), 1.13(d, 6H), 0.90(m, 12H) and 0.27 ppm (d, 6H).

**I. Synthesis of chlorido(2-(phenylazo)-3-methylpyridine)(2,6-bis(2,6-diisopropylphenylimino methyl)pyridine)ruthenium(II) perchlorate, RuL2-3mazpy.** RuL2(50 mg, 0.0756 mmol, 1 Eq), 3-mazpy (22.37 mg, 0.1134 mmol, 1.5 Eq), LiCl (50 mg, 1.18 mmol) and triethylamine (0.015 mL). Yield: 99% (0.0749 mmol, 66.43 mg). Elemental analysis for $RuC_{43}H_{50}N_6Cl_2O_4$: Calculated (%): C, 58.23; N, 9.48 and H, 5.68. Found (%): C, 58.38; N, 9.35 and H, 5.48. ESI-MS: m/z=804.90, $[RuL2\text{-}3mazpy - ClO_4 + H_2O]^+$, where calculated m/z=805.45; m/z=786.88, $[RuL2\text{-}3mazpy - ClO_4]^+$, 100%, where calculated m/z=787.43. IR: 3100-2800, 1586, 1500-1435, 1400-1366, 1312, 1300, 1242, 1090, 1001-899, 801-748, 682, 622, 480, 408 and 339 $cm^{-1}$. UV-Vis in acetonitrile ($\lambda_{max}(\log\varepsilon_M)$): 229(4.56), 347(4.13) and 563(3.92). $^1H$ NMR (300 MHz, deuterated acetonitrile, 294 K, s=singlet, d=doublet, t=triplet and m=multiplet): $\delta$=9.25(d, 1H), 8.78(m, 4H), 8.52(t, 1H), 7.92(d, 1H), 7.77(m, 3H), 7.66(t, 1H), 7.54(t, 2H), 7.06(m, 4H), 6.89(d, 2H), 3.81(m, 2H), 2.67(s, 3H),1.69(m, 2H), 1.15(d, 6H), 0.96(d, 6H), 0.62(d, 6H), and 0.45 ppm (d, 6H).

**J. Synthesis of chlorido(1,10-phenanthroline)(2,6-bis(2,6-diisopropylphenyliminomethyl) pyridine)ruthenium(II) perchlorate, RuL2-phen.** RuL2(50 mg, 0.0756 mmol, 1 Eq), phen (20.44 mg, 0.1134 mmol, 1.5 Eq), LiCl (50 mg, 1.18 mmol) and triethylamine (0.015 mL). Yield: 52 % (0.0392 mmol, 34.11 mg). X-ray quality crystals were obtained by slow evaporation of a concentrated solution of RuL2-phen in acetonitrile. Elemental analysis for $RuC_{43}H_{47}N_5Cl_2O_4$: Calculated (%): C, 59.37; N, 8.05 and H, 5.45. Found (%): C, 59.28; N, 7.82 and H, 5.19. ESI-MS: m/z=769.84, $[RuL2\text{-}phen - ClO_4]^+$, 100%, where calculated m/z=770.40. IR: 3100-2800, 1575-1558, 1506-1365, 1204, 1080, 840, 804-720, 621, 589-480, 418, and 328 $cm^{-1}$. UV-Vis in acetonitrile ($\lambda_{max}(\log\varepsilon_M)$): 267(4.53) and 494(3.98). $^1H$ NMR (300 MHz, deuterated acetonitrile, 294 K, s=singlet, d=doublet, t=triplet and m=multiplet): $\delta$=10.10(d, 1H), 8.77(s, 2H), 8.67(m, 5H), 8.21(m, 4H), 7.93(dd, 1H), 6.92(m, 4H), 6.58(d, 2H), 4.18(m, 2H), 1.33(m, 2H), 1.16(d, 6H), 0.92(d, 6H), 0.72(d, 6H) and -0.23 ppm (d, 6H).

**K. Synthesis of chlorido(2-picolinate)(2,6-bis(2,6-diisopropylphenyliminomethyl)pyridine) ruthenium(II) perchlorate, RuL2-pic.** RuL2(100 mg, 0.151 mmol, 1 Eq), 2-picolinic acid (18.62 mg, 0.151 mmol, 1.0 Eq), LiCl (38.48 mg, 1.91 mmol) and triethylamine (0.035 mL). Yield: 68 % (0.102 mmol, 72.06 mg). Elemental analysis for $RuC_{37}H_{43}N_4ClO_2$: Calculated (%): C, 62.39; N, 7.87 and H, 6.08. Found (%): C, 62.40; N, 7.83 and H, 5.95. ESI-MS: m/z=712.81, $[RuL2\text{-}pic + H^+]^+$, 100%, where calculated m/z=713.30. IR: 3100-2800, 1656-1634, 1602, 1464-1436, 1381, 1329, 1267, 1164, 1060, 804, 770-736, 692, 595, 452, and 325 $cm^{-1}$. UV-Vis in acetonitrile ($\lambda_{max}(\log\varepsilon_M)$): 236(4.30), 307(3.87) and 501(3.81). $^1H$ NMR (300 MHz, deuterated acetonitrile, 294 K, s=singlet, d=doublet, t=triplet and m=multiplet): $\delta$=9.89(d, 1H), 8.74(s, 2H), 8.30(d, 2H), 7.75(m, 3H), 7.47(d, 1H), 6.99(m, 4H), 6.87(d, 2H), 3.96(m, 2H), 2.46(m, 2H), 1.05(m, 18H) and 0.88 ppm (d, 6H).

**L. Synthesis of chlorido(2-(tolylazo)pyridine)(2,6-bis(2,6-diisopropylphenyliminomethyl) pyridine)ruthenium(II) perchlorate, RuL2-tazpy.** RuL2(50 mg, 0.0756 mmol, 1 Eq), tazpy (22.37 mg, 0.1134 mmol, 1.5 Eq), LiCl (50 mg, 1.18 mmol) and triethylamine (0.015 mL). Yield: 49 % (0.03670 mmol, 32.55 mg). Elemental analysis for $RuC_{43}H_{50}N_6Cl_2O_4$: Calculated (%): C, 58.23; N, 9.48 and H, 5.68. Found (%): C, 57.75; N, 9.23 and H, 5.67. ESI-MS: m/z=804.83, $[RuL2\text{-}tazpy - ClO_4 + H_2O]^+$, where calculated m/z=805.45; m/z=786.85, $[RuL2\text{-}tazpy - ClO_4]^+$, 100%, where calculated m/z=787.43. IR: 3100-2800, 1572-1596, 1506, 1460-1436, 1386-1300, 1249, 1081, 960-897, 800-730, 668, 622, 424 and 316 $cm^{-1}$. UV-Vis in acetonitrile ($\lambda_{max}(\log\varepsilon_M)$): 313(4.18), 344(4.15) and 546(3.71). $^1H$ NMR (300 MHz, deuterated acetonitrile, 294 K, s=singlet, d=doublet, t=triplet and m=multiplet): $\delta$=9.02(s, 2H), 8.87(d, 1H), 8.65(d, 2H), 8.32(t, 1H), 7.83(m, 5H), 7.57(d,

1H), 7.21(m, 4H), 7.05(dd, 2H), 6.92(d, 1H), 4.30(m, 2H), 2.45(s, 3H), 1.85(m, 2H), 1.24(d, 6H), 0.99(d, 6H), 0.77(d, 6H) and 0.42 ppm (d, 6H).

*Caution*: perchlorate salts of metal complexes with organic ligands are potentially explosive. Only small amounts of the compound should be prepared and handled with great care.

## 5.3 Results and discussion

### 5.3.1 Synthesis and characterization of bis(arylimino)pyridine-Ru(II) compounds

The direct reaction of $[RuLxCl_3]\cdot nH_2O$ (Lx=L1: 2,6-bis(2,4,6-trimethylphenyl iminomethyl)pyridine or L2: 2,6-bis(2,6-diisopropylphenyliminomethyl)pyridine and n=0,1) with several bidentate ligands was carried out and the schematic representation is depicted in figure 5.1. Using the appropriate molar ratios, in refluxing ethanol:water (70:30), containing triethylamine as reducing agent, and a little excess of LiCl in order to prevent $Cl^-$ dissociation in the final products, two new families of Ru(II) compounds were produced in good-to-moderate yields. Similar synthetic procedures have been employed in the synthesis of Ru(II)-terpyridine analogues [48-55].

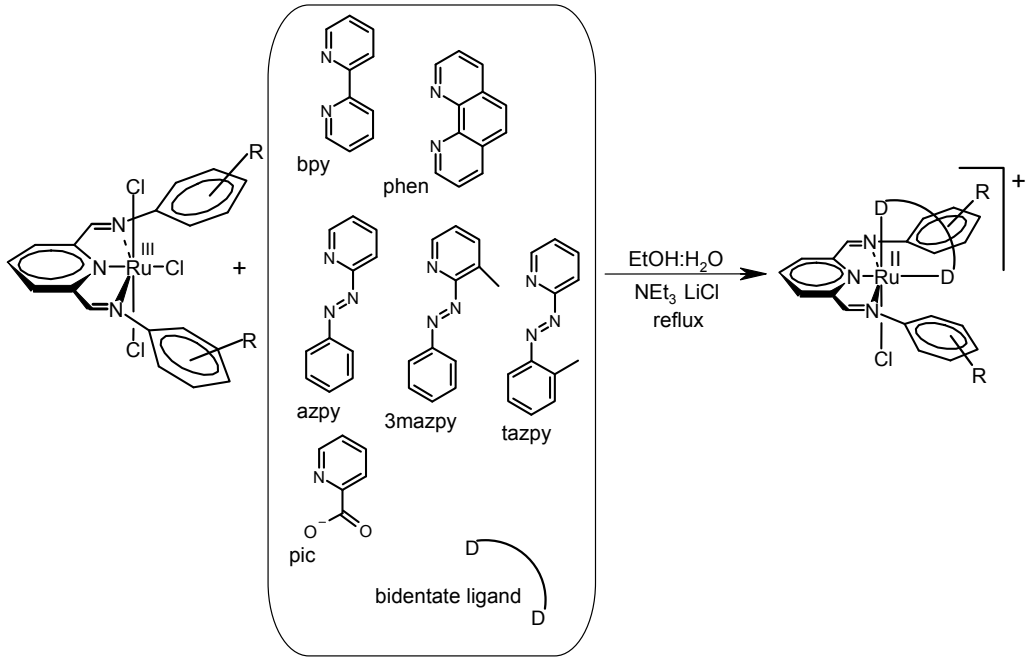


**Figure 5.1** Schematic representation of the synthesis of the Ru(II) complexes included in this chapter. The abbreviations for the bidentate ligands are also included. The substituents in the phenyl moiety in the tridentate ligands have been omitted for clarity purposes and corresponds to L1(2,6-bis(2,4,6-trimethylphenyliminomethyl)pyridine) or L2(2,6-bis(2,6-diisopropylphenyliminomethyl)pyridine).

The perchlorate salts of the 12 new compounds contain 1:1 metal to bis(arylimino)pyridine ligand ratio, one bidentate ligand ((Npy-Npy)-donors as phen or bpy; (Npy-Nazo)-donors as azpy, 3mazpy or tazpy; or (Npy-O)-donors as 2-picolinate) and one chloride ligand, completing the octahedral arrangement. All the compounds described here have been characterized by a variety of techniques, including elemental analysis, ESI-MS spectrometry, UV-Vis, IR, EPR and $^1$H NMR spectroscopy. In addition the solid-state molecular structures of compounds RuL1-pic, RuL2-bpy and RuL2-phen were determined by X-ray crystallography.

The elemental analyses were found consistent with the proposed structures and they also proved the purity of the samples. The compounds are partially soluble in water and ethanol, but they are highly soluble in polar organic solvents, such as methanol, acetonitrile, acetone, dmso and dmf.

Bis(arylimino)pyridine ligands are coordinated in a meridional fashion. The group of three 2-(arylazo)pyridine ligands, which differ with respect to the location of a methyl moiety in the pyridine and phenyl ring, has been selected in order to slightly modify the chemical properties of the Ru(II)-complexes. As these ligands are not symmetric, the formation of two isomers could be

expected. However, in practice only one isomer has been isolated as has been confirmed by $^1$H NMR and X-ray diffraction studies. This observation is consistent with reports of similar Ru(II)-tpy derivatives and azopyridine-bidentate ligands [51, 56]. The same isomerisation would be expected in case of the picolinic acid derivatives, but again, just one isomer, thermodynamically stable, was observed.

The azo functionalities have stronger $\pi$-acidity than the imino and pyridine ones, stabilizing lower oxidation states of Ru [57-59]. The carboxylate oxygen is also a hard donor and well known for stabilizing higher oxidation states [60, 61].

Table 5.1 lists the analytical data for the starting Ru(III) compounds and their Ru(II) analogues. For a complete overview refer to the experimental section.

**Table 5.1** Analytical and physical data of the Ru(II) complexes reported here.

| Compound | MW | Colour | Yield | Found(calc.)(%) | | |
|---|---|---|---|---|---|---|
| | | | (%) | C | N | H |
| Ru(III)L1.$H_2O$ | 594.95 | Dark green | 92 | 50.37(50.47) | 7.05(7.06) | 5.03(4.91) |
| Ru(III)L2 | 661.10 | Dark brown | 81 | 56.19(56.32) | 6.40(6.36) | 6.26(5.95) |
| RuL1-azpy | 806.71 | Dark purple-brown | 69 | 53.35(53.60) | 10.32(10.42) | 4.90(4.75) |
| RuL1-bpy | 779.68 | Dark red-brown | 72 | 54.02(53.92) | 9.11(8.98) | 4.69(4.78) |
| RuL1-3mazpy | 802.72 | Dark purple-brown | 33 | 55.57(55.36) | 10.66(10.47) | 4.81(4.77) |
| RuL1-phen | 785.69 | Dark red-brown | 56 | 56.33(56.56) | 8.81(8.91) | 4.50(4.49) |
| RuL1-pic | 628.12 | Dark purple brown | 73 | 58.85(59.28) | 8.59(8.92) | 4.75(4.97) |
| RuL1-tazpy | 802.72 | Dark purple brown | 93 | 55.10(55.36) | 10.47(10.47) | 4.55(4.77) |
| RuL2-azpy | 872.86 | Dark purple brown | 74 | 57.24(57.79) | 9.51(9.63) | 5.77(5.54) |
| RuL2-bpy | 845.83 | Dark red-brown | 81 | 58.81(58.22) | 8.50(8.28) | 5.52(5.60) |
| RuL2-3mazpy | 886.88 | Dark purple brown | 99 | 58.38(58.23) | 9.35(9.48) | 5.48(5.68) |
| RuL2-phen | 869.85 | Dark red-brown | 52 | 59.28(59.37) | 7.82(7.87) | 5.19(5.45) |
| RuL2-pic | 712.30 | Dark purple brown | 68 | 62.40(62.39) | 7.83(7.87) | 5.95(6.08) |
| RuL2-tazpy | 886.88 | Dark purple brown | 49 | 57.75(58.23) | 9.23(9.48) | 5.67(5.68) |

**A) X-ray Crystallography**. Crystals suitable for the studies were obtained by slow evaporation of a concentrated solution of the compounds, RuL1-pic, RuL2-bpy and RuL2-phen in acetonitrile. The dark purple (RuL1-pic), and dark orange blocks (RuL2-bpy and RuL2-phen) were mounted on a glass fibre. The structures of the ruthenium complexes are ordered and their complex cation units are shown in Figures 5.2, 5.3 and 5.4. Table 5.2 and 5.3 contain the crystallographic data and selected bond lengths and angles for each compound. They belong to the same space group as other related Ru(II)-bis(arylimino)pyridine compounds reported in the literature [62] but also share close similarities with the Ru(II)-tpy systems [63]. The numbering scheme is proposed in order to keep consistency with related structures described in previous chapters.

**Table 5.2** Crystallographic data for RuL1-pic, RuL2-bpy and RuL2-phen.

| Abbreviation: | **RuL1-pic** | **RuL2-bpy** | **RuL2-phen** |
|---|---|---|---|
| empirical formula | $C_{31}H_{31}N_4O_2ClRu$ | $C_{41}H_{47}N_5ClRu(ClO_4)$ | $C_{43}H_{47}N_5ClRu(ClO_4)$ |
| Fw | 628.12 | 845.81 | 869.83 |
| crystal symmetry | monoclinic | monoclinic | monoclinic |
| Space group | $P2_1/c$ (No. 14) | $P2_1/c$ (No. 14) | $P2_1/c$ (No. 14) |
| $a$, Å | 8.0751(3) | 13.2444(4) | 14.1035(2) |
| $b$, Å | 25.4734(8) | 15.0132(5) | 15.0163(3) |
| $c$, Å | 14.7742(5) | 26.5417(10) | 26.4919(4) |
| $\alpha, \beta, \gamma$ (°) | 90,111.606(3),90 | 90, 119.389(2), 90 | 90, 120.11(10), 90 |
| $V$, Å$^3$ | 2825.53(18) | 4598.4(3) | 4843.50(15) |
| $Z$ | 4 | 4 | 4 |
| $T$, K | 150(2) | 150(2) | 150(2) |
| $\rho_{calcd}$, g/cm$^3$ | 1.477 | 1.222 | 1.190 |
| $\mu$, mm$^{-1}$ | 0.69 | 0.50 | 0.47 |
| $R1$[a] | 0.023 | 0.030 | 0.032 |
| $wR2$[b] | 0.054 | 0.072 | 0.079 |
| GOF | 1.04 | 1.06 | 1.06 |
| $\Delta\rho_{max}$, e Å$^{-3}$ | 0.40 | 0.52 | 0.64 |
| $\Delta\rho_{min}$, e Å$^{-3}$ | -0.47 | -0.34 | -0.78 |

[a] $R1 = \Sigma\,||F_o| - |F_c||/\Sigma|F_o|$. [b] $wR2 = \{\Sigma[w(F_o^2-F_c^2)^2]/\Sigma[w(F_o^2)^2]\}^{1/2}$

These results confirm not only the chemical structure of RuL1-pic, RuL2-bpy and RuL2-phen, but indirectly also confirm the chemical structure of RuL1 and RuL2, as starting materials.

In the structures of RuL1-pic, RuL2-bpy and RuL2-phen, the Ru(II) ion is coordinated to the bis(arylimino)pyridine tridentate ligand (L1 or L2), a bidentate ligand (2-picolinate (N,O), bipyridine (N,N) or phenanthroline (N,N)) and a monodentate chloride in a distorted octahedral geometry. The bis(arylimino)pyridine moiety is mainly planar through the plane of coordination and it coordinates in a *mer* fashion with the bidentate ligands in *cis* orientation [64]. It is noted that the planes of the substituted-phenyl rings in L1 or L2, are oriented essentially orthogonal to the plane of the backbone (78.33° for RuL1-pic, 78.14° for RuL2-bpy and 82.52° for RuL2-phen), as observed in other, related iron, cobalt and ruthenium systems [62, 65]. Similar data have been previously described for RuL1-2(9EtGua) (see Chapter 4). The *ortho*-methyl substituents in the phenyl rings of L1 are not bulky enough to protect the metal centre in RuL1-pic, but the *ortho*-isopropyl substituents are bulkier and tend to protect the Ru(II) centre. This effect has been observed for other metal centres as well [65]. Despite of the bulkiness of the isopropyl moiety, the orientation of the substituted-phenyl rings is not substantially modified.

**Table 5.3** Selected geometric parameters (Angstroms, degrees) for RuL1-pic, RuL2-bpy and RuL2-phen.

| **Distances (Angstroms)** | | | | | |
|---|---|---|---|---|---|
| **RuL1-pic** | | **RuL2-bpy** | | **RuL2-phen** | |
| Ru1-Cl1 | 2.3889(5) | Ru1-Cl1 | 2.3835(5) | Ru1-Cl1 | 2.3982(5) |
| Ru1-O1 | 2.0816(13) | | | | |
| Ru1-N1 | 1.9366(15) | Ru1-N1 | 1.9411(16) | Ru1-N1 | 1.9469(19) |
| Ru1-N2 | 2.1027(15) | Ru1-N2 | 2.1610(15) | Ru1-N2 | 2.0817(17) |
| Ru1-N3 | 2.0664(15) | Ru1-N3 | 2.0762(15) | Ru1-N3 | 2.1677(17) |
| Ru1-N4 | 2.0972(15) | Ru1-N4 | 2.0489(16) | Ru1-N4 | 2.0423(18) |
| | | Ru1-N5 | 2.0910(16) | Ru1-N5 | 2.0909(19) |
| N1- C1 | 1.365(2) | N1- C1 | 1.355(2) | N1- C1 | 1.357(3) |
| N2-C6 | 1.309(2) | N2-C6 | 1.295(3) | N2-C6 | 1.293(3) |
| N2-C7 | 1.453(2) | N2-C7 | 1.461(2) | N2-C7 | 1.459(3) |
| N3-C16 | 1.309(2) | N3-C19 | 1.297(3) | N3-C19 | 1.296(3) |
| C1-C2 | 1.396(3) | C1-C2 | 1.388(3) | C1-C2 | 1.388(4) |
| C1-C6 | 1.448(3) | C1-C6 | 1.453(3) | C1-C6 | 1.452(3) |
| C7-C8 | 1.408(3) | C7-C8 | 1.401(3) | C7-C8 | 1.405(3) |
| C26-N4 | 1.352(2) | C32-N4 | 1.349(2) | C32-N4 | 1.335(3) |
| C26-C27 | 1.387(3) | C32-C33 | 1.375(3) | C32-C33 | 1.397(4) |
| C30-C31 | 1.517(2) | C36-C37 | 1.466(3) | C36-C39 | 1.426(3) |
| C31-O1 | 1.294(2) | | | | |
| C31-O2 | 1.229(2) | | | | |
| **Angles ( Degrees)** | | | | | |
| **RuL1-pic** | | **RuL2-bpy** | | **RuL2-phen** | |
| Cl1-Ru1-O1 | 174.45(4) | | | | |
| Cl1-Ru1-N1 | 83.00(4) | Cl1-Ru1-N1 | 91.93(5) | Cl1-Ru1-N1 | 91.98(5) |
| Cl1-Ru1-N2 | 90.36(4) | Cl1-Ru1-N2 | 85.29(4) | Cl1-Ru1-N2 | 93.54(5) |
| Cl1-Ru1-N3 | 92.89(4) | Cl1-Ru1-N3 | 92.35(4) | Cl1-Ru1-N3 | 85.21(5) |
| Cl1-Ru1-N4 | 96.50(4) | Cl1-Ru1-N4 | 170.96(5) | Cl1-Ru1-N4 | 171.40(6) |
| | | Cl1-Ru1-N5 | 95.11(4) | Cl1-Ru1-N5 | 93.71(5) |
| O1-Ru1-N1 | 102.45(6) | | | | |
| O1-Ru1-N2 | 89.74(5) | | | | |
| O1-Ru1-N4 | 78.10(5) | | | | |
| N1-Ru1-N2 | 78.45(6) | N1-Ru1-N2 | 77.63(6) | N1-Ru1-N2 | 78.41(7) |
| N1-Ru1-N3 | 78.71(6) | N1-Ru1-N3 | 78.45(6) | N1-Ru1-N3 | 77.75(7) |
| N1-Ru1-N4 | 177.27(6) | N1-Ru1-N4 | 95.59(6) | N1-Ru1-N4 | 95.40(7) |
| | | N1-Ru1-N5 | 171.15(6) | N1-Ru1-N5 | 171.72(6) |
| N2-Ru1-N3 | 156.34(6) | N2-Ru1-N3 | 155.86(6) | N2-Ru1-N3 | 156.07(7) |
| N2-Ru1-N4 | 104.25(6) | N2-Ru1-N4 | 91.41(6) | N2-Ru1-N4 | 92.26(7) |
| | | N2-Ru1-N5 | 108.26(6) | N2-Ru1-N5 | 95.23(7) |
| N3-Ru1-N4 | 98.65(6) | N3-Ru1-N4 | 94.06(6) | N3-Ru1-N4 | 92.05(6) |
| | | N3-Ru1-N5 | 95.89(6) | N3-Ru1-N5 | 108.71(7) |
| | | N4-Ru1-N5 | 77.91(6) | N4-Ru1-N5 | 79.43(7) |
| C1-N1-C5 | 121.14(15) | C1-N1-C5 | 120.62(17) | C1-N1-C5 | 121.04(19) |
| C6-N2-C7 | 115.30(15) | C6-N2-C7 | 114.87(15) | C6-N2-C7 | 118.69(18) |
| C26-N4-C30 | 118.15(15) | | | | |
| | | C32-N4-C36 | 118.41(17) | C32-N4-C36 | 117.74(19) |
| | | C37-N5-C41 | 118.21(17) | C39-N5-C43 | 117.4(2) |

In all the octahedral complexes, a major distortion arises via the coordination with the tridentate ligands (L1 and L2), where the trans bite angles are 156.34(4)°, 155.86(6)° and 156.07(7)° for RuL1-pic, RuL2-bpy and RuL2-phen, respectively; similar behaviour has been observed in the Ru(II)-terpyridine systems (158-159°) [54, 66]. This angle is considerably smaller than the ideal angle of 180° and the same effect in closely related Ru(II)-bis(arylimino)pyridine compounds is already reported in the literature (bite angle 155-158°) [62, 67]. The Cl-Ru-Npy (tridentate ligand) angles of 91.93(5)° for RuL2-bpy and 91.98(5)° for RuL2-phen. These results indicate a moderate deviation from the expected 90° angle. In contrast the 83.00(4)° angle in RuL1-pic indicates significant deviation from the 90° angle. The Ru-Npy bond lengths in the tridentate moiety (1.937(15) Å for RuL1-pic, 1.941(16) Å for RuL2-bpy and 1.947(19) Å for RuL2-phen) are shorter than the Ru-Nimino bond lengths (2.066(15)-2.103(15) Å for RuL1-pic, 2.080(15)-2.161(15) Å for RuL2-bpy and 2.082(17)-2.168(17) Å for RuL2-phen). This shortening is explained to help in the optimization of the chelation of the tridentate bis(arylimino)pyridine ligands, as observed in case of coordination of tpy, where the central metal-Npyr bond shortens, while the terminal ones lengthen by approximately 0.1 Å [54, 63, 66, 68]. Worthy of consideration is the slight, but significant difference (0.03-0.08 Å approximately) between the two Ru-Nimino distances in each molecule which must be generated by the octahedral distortion. Similar difference in the lengths has been observed in [Ru(2,6-bis(1,4-methoxyphenyliminoethyl)pyridine)($CH_3CN$)$Cl_2$] [62]. The double bond character of the imino linkage N2-C6 is retained (1.309(2) Å for RuL1-pic, 1.295(3) Å for RuL2-bpy and 1.293(3) Å for RuL2-phen) although a slightly longer length is observed, when comparing with the free ligands L1 (1.2493(18) Å) and L2 (1.2686(17) Å). RuL1-pic shows the longest C=Nimino distance.

Other important feature is the reduction in the C1-C6 bond distance upon coordination (1.448(3) Å for RuL1-pic, 1.453(3) Å for RuL2-bpy and 1.452(3) Å for RuL2-phen, again, when comparing with the free ligands (1.4733(18) Å for L1 and 1.476(18) Å for L2).

The Ru(II)-Cl distances are in the range 2.3835-2.3889 Å and similar values have been found in comparable ruthenium complexes [63, 68-70].

For RuL1-pic (figure 5.2), the Ru-Npy distance in the picolinate ligand coordinated is 2.0972(15) Å which is comparable to other compounds reported in literature (2.025-2.078 Å) [37, 71-73]. For instance, the Ru-Npy for the 2-picolinate and the Ru-O bond distances in [Ru(tpy)(dmso)(pic)]$^+$ are 2.101(2) and 2.085(2) Å, respectively. The Ru-O bond length, in RuL1-pic, for the same ligand (pic), around 2.0816 (13) Å, could be explained by the trans effect imposed by the chloride ligand as previously observed in similar reported [Ru(pic)$_2$(NO)($CH_3CN$)]$^+$ systems [72]. In the same 2-picolinate moiety, the two C-O bonds of the carboxylate group, which correspond, to the C-O and C=O bonds, are also evident in the structure of RuL1-pic. The O1-C31 bond length corresponds to a single bond (1.294(2) Å), while the O2-C31 bond length corresponds to a double bond (1.229(2) Å), and belongs to the oxygen which is not coordinated to the Ru(II) centre.

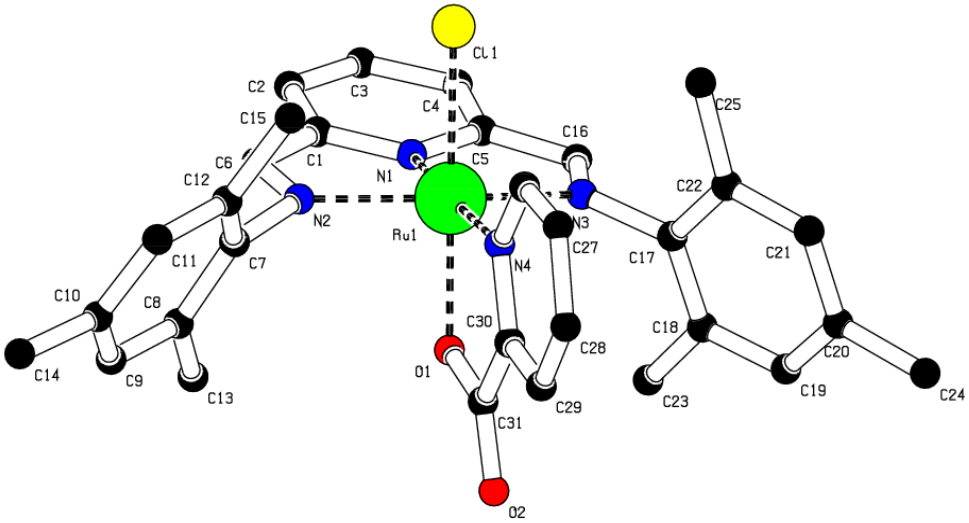


**Figure 5.2** PLATON projection of the cation unit of RuL1-pic at 150 K. The numbering scheme is proposed in order to have consistency with previous chapters. The hydrogen atoms have been omitted for clarity.

The angle Cl1-Ru1-O1(174.45(4)°) is slightly deviated from the normal angle for an octahedral conformation (180°), while the bite angle of 2-picolinate is around 78.10(5) and it is consistent with previously reported data [37].

For the RuL2-bpy and RuL2-phen X-ray structures (figure 5.3 and 5.4), some relevant features are observed. The bipyridine and phenanthroline ligands are planar and symmetric by themselves. Once coordinated to the Ru(II) complexes, the chloride ligand is necessarily *trans* to one of the bipyridine or phenanthroline nitrogen atoms. The Ru-Npy bond distances of the two bipyridine or phenanthroline nitrogen atoms within each compound, are slightly different (difference of 0.0421 for bpy and 0.0486 for phen) with a longer Ru-Npy bond, which is *cis* to the chloride ligand and *trans* to the central pyridine of the bis(arylimino)pyridine ligand. The shorter Ru-Npy bond in the bidentate ligand, is *cis* to the central pyridine ring in the tridentate ligand (L1 or L2). These results differ from previously reported observations where the Ru-Npy bond from the bipyridine, which is *trans* to a central pyridine (terpyridine for instance) in a tridentate ligand, are normally longer and represent a typical feature in $[Ru(tpy)(bpy)L]^{2+}$ complexes [63, 66].

This difference in length could be explained by interligand steric interactions between L1 or L2 and the bidentate ligands, rather than by a trans effect of the central nitrogen of the tpy ligand [54, 74, 75].

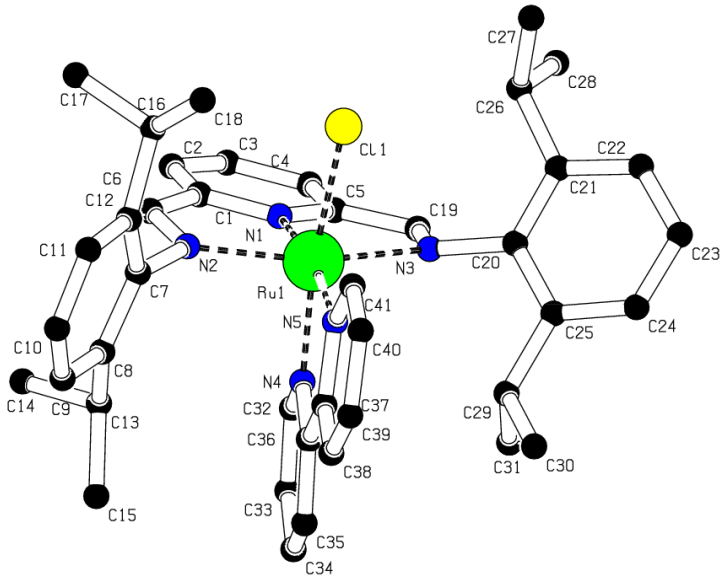


**Figure 5.3** PLATON projection of the cation unit of RuL2-bpy at 150 K. The numbering scheme is proposed in order to have consistency with previous chapters. The hydrogen atoms and the counterion have been omitted for clarity reasons.

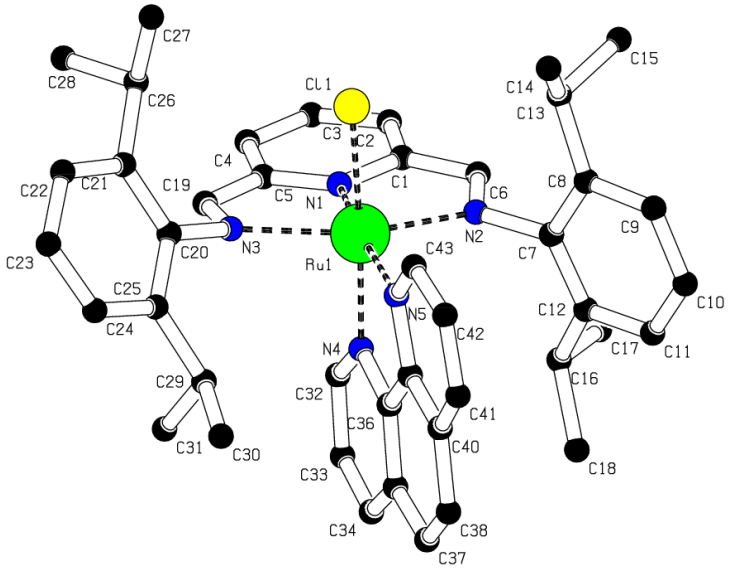


**Figure 5.4** PLATON projection of the cation unit of RuL2-phen at 150 K. The numbering scheme is proposed in order to have consistency with previous chapters. The $ClO_4^-$ counter anion and hydrogen atoms have been omitted for clarity.

**B) ESI-MS.** The mass spectra were measured in the positive mode and in the range of m/z=200-1200. Ions containing ruthenium presents a clearly visible metal isotope pattern arising from the distribution, $^{96}$Ru 5.52, $^{98}$Ru 1.88, $^{99}$Ru 12.7, $^{100}$Ru 12.6, $^{101}$Ru 17, $^{102}$Ru 31.6 and $^{104}$Ru 18.7% [54, 76]. For all the perchlorate salts of the Ru(II) compounds studied, the loss of the perchlorate is the dominant ionization process observed, this generates a singly charged Ru(II) ion. The positive ion spectra of the compounds show mainly one major ion. In some cases an ion, which could be explained as the association of water to the positively charged complex, is also observed in the spectra. This fragmentation pattern in the ESI mass spectra of each complex strongly supports the proposed formulation of the complexes. For RuL1-pic and RuL2-pic, the major ions observed correspond to the addition of one proton and the peaks exhibit the correct isotopomer distribution. The mass spectra of RuL1-phen and RuL2-3mazpy are shown in figures 5.5 and 5.6 respectively.

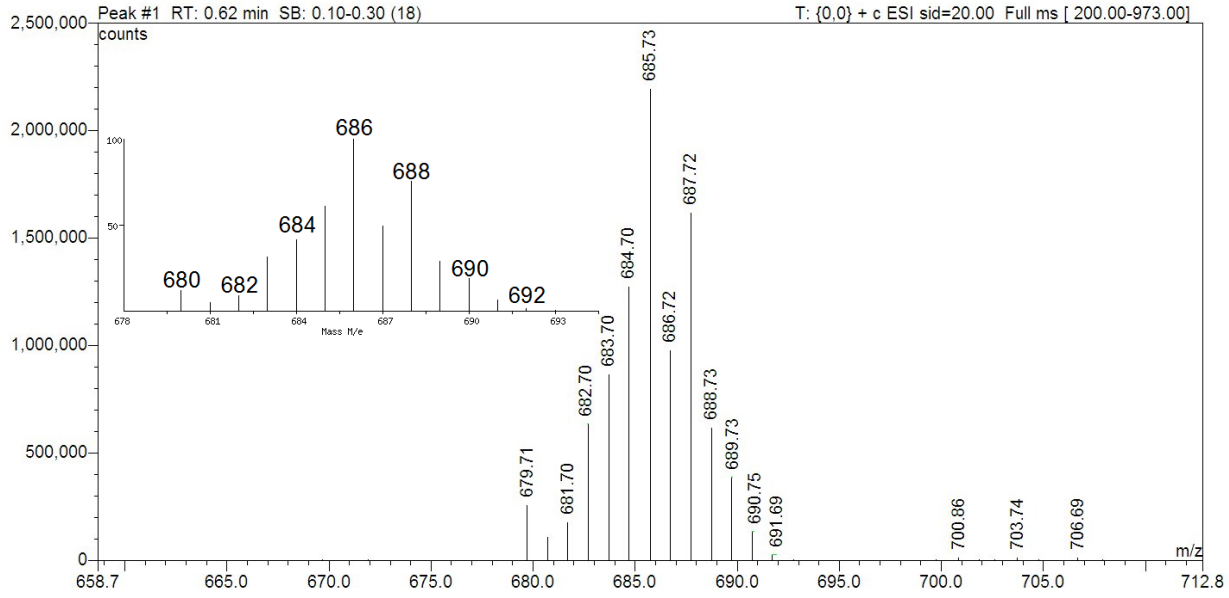


**Figure 5.5** ESI-MS positive ion spectrum of RuL1-phen (m/z in Da). See experimental section for calculated data. In the inset: The calculated spectrum for the cation of RuL1-phen (m/z in Da).

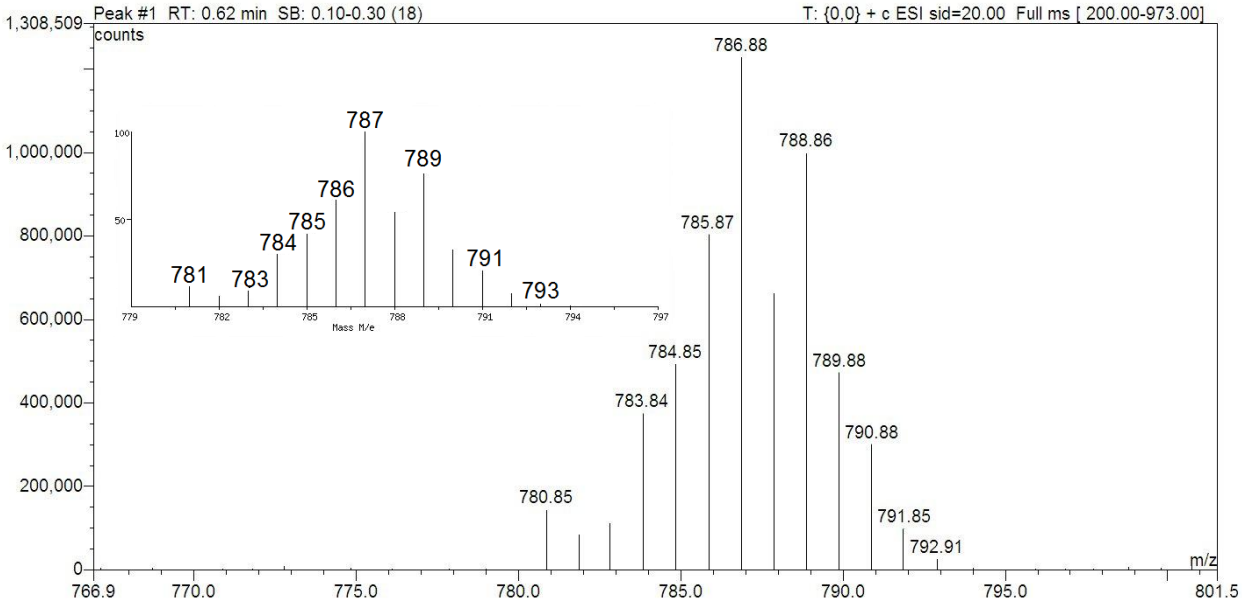


**Figure 5.6** ESI-MS positive ion spectrum of RuL2-3mazpy (m/z in Da). See experimental section for calculated data. In the inset: The calculated spectrum for the cation of RuL2-3mazpy is shown in the inset.

**C) IR.** From IR studies, several changes were observed in the spectra of the twelve Ru(II) compounds when comparing with the corresponding spectra obtained from the starting

reagents, RuL1 and RuL2. Table 5.4 summarizes the most important IR peaks, the corresponding assignment and frequencies in the mid-IR region, confirming the presence of the bis-(arylimino)pyridine ligand, the bidentate ligand (azpy, bpy, 3mazpy, phen, pic and tazpy) and the chloride ligand all coordinated to Ru(II). A sharp vibration peak assigned to the ν(Ru-Cl) stretching mode was observed around 320 $cm^{-1}$ in all cases and the values are in accordance with the proposed structures [63, 66, 77]. The HC=N(imino)bond stretching vibrations of the tridentate ligands are present and the shift is associated to metal coordination. The strong band around 1595 $cm^{-1}$ in the Ru(III) starting material, is shifted to higher frequency in the analogues Ru(II) complexes, with the biggest shifts for RuL1-3mazpy and RuL2-azpy. These shifts support the participation of the imino nitrogen in binding to the metal ion [68, 78]. The weak bands between 3200 and 2800 $cm^{-1}$ are related to (C-H) modes of vibration. Also, some weak bands located between 2000-1750 $cm^{-1}$ can be assigned to overtones of the aromatic rings. The bands appearing at 374.3 for RuL1 and 390 for RuL2 can be attributed to the ν (M-N) bond vibration of the pyridine nitrogen. For the Ru(II) compounds, this vibration peaks present blue shifts and they are consistent with the proposed changes in the structures. In the compounds RuL1 and RuL2, the bands appearing around 600 $cm^{-1}$ can be assigned to the ν(M-N) bond vibration of the imino nitrogen atoms. For the Ru(II) compounds, this vibration mode presents a red shift. Finally the strong peaks around 325 $cm^{-1}$ are attributed to the Ru-Cl stretching bond vibration, values that are also comparable to other Ru(II) complexes with chloride ligands[51, 63].

Two intense vibrations observed around 1090 and 622 $cm^{-1}$ are attributed to the presence of the $ClO_4^-$ anion [51, 63, 79]. As expected they are not present in RuL1-pic and RuL2-pic.

**Table 5.4** IR assignment of the Ru(II)-complexes spectra. Selected peaks only.

| Frequencies ($cm^{-1}$) | Peaks ν (HC=N) | ν (C=N)pyr | ν Ru-Npy | ν Ru-Nimin | νRu-Cl | $\nu OCO_{as}$ | $\nu ClO_4^-$ | $\nu ClO_4^-$ |
|---|---|---|---|---|---|---|---|---|
| RuL1 | 1595.5 | 1540 | 374.3 | 607-586 | 325 | | - | - |
| RuL1-azpy | 1599 | 1500-1450 | 388 | 590-544 | 318 | | 1090 | 622 |
| RuL1-bpy | 1600 | 1505-1418 | 384 | 594 | 324 | | 1090 | 622 |
| RuL1-3mazpy | 1650 | 1650-1558 | 376 | - | 326 | | 1082 | 622 |
| RuL1-phen | 1599 | 1599-1506 | 382 | 524-470 | 328 | | 1080 | 622 |
| RuL1-pic | 1602 | - | 334 | 601-590 | 324 | 1635 | - | - |
| RuL1-tazpy | 1599 | 1520 | 388 | - | 328 | | 1081 | 622 |
| RuL2 | 1590 | 1550-1540 | 390 | 593 | 328 | | - | - |
| RuL2-azpy | 1615 | 1615-1580 | 410 | 590 | 322 | | 1090 | 622 |
| RuL2-bpy | 1604 | 1506-1420 | 408 | 588 | 316 | | 1089 | 622 |
| RuL2-3mazpy | 1586 | 1500-1435 | 408 | - | 339 | | 1090 | 622 |
| RuL2-phen | 1575 | 1575-1558 | 418 | 589-480 | 328 | | 1080 | 621 |
| RuL2-pic | 1602 | - | 452 | 595 | 325 | 1656 | - | - |
| RuL2-tazpy | 1596 | 1596-1572 | 424 | - | 316 | | 1081 | 622 |

The N=N stretching frequency of the coordinated 2-(arylazo)pyridine ligands is lowered (around 1320 $cm^{-1}$) compared to that of the free ligand (around 1420 nm, see also chapter 2).

The strong band in the region of 1650-1620 $cm^{-1}$ is assigned to the coordinated carboxylate group in the 2-picolinate ligand [48, 80, 81] and as expected is just observed in case of RuL1-pic and RuL2-pic. In 2-picolinic acid, this vibration is observe around 1700 $cm^{-1}$, and then the decrease in frequency is due to coordination [82].

**D) Electronic absorption properties.** The absorption spectra of the complexes, in the UV-Vis region, were recorded using a Varian CARY 50 UV/VIS spectrophotometer operating at room temperature, with freshly prepared acetonitrile solutions (around 0.03 mM), due to the poor solubility in water of these ruthenium compounds. The spectra of the Ru(II)L1 and Ru(II)L2 derivatives (figures 5.7.and 5.8) are characterized by intense peaks in the region that comprises 200-700 nm. The spectra in the visible region are dominated by the expected $d\rightarrow\pi^*$ MLCT bands and in the UV region by ligand-centred $\pi\rightarrow\pi^*$-transitions from tridentate and bidentate ligands, and which are clearly overlapping. The transition bands at 317 nm ($\log\varepsilon_M$=3.74) and 390 nm ($\log\varepsilon_M$=3.80), for Ru(III)L1; and at 293 nm ($\log\varepsilon_M$=3.78) and 387 nm ($\log\varepsilon_M$=3.72), for Ru(III)L2,

present a blue shift after reduction of the Ru centre (figure 5.7 and 5.8). The transitions observed in the visible region in the spectra of these compounds, are comparable to other Ru(II) complexes that involve nitrogen donor molecules [74, 83-85]. Several charge transfer $d\pi(Ru(III))\rightarrow\pi^*(L)$-absorptions are observed in the visible region of the spectra. RuL1-bpy, RuL1-phen, RuL2-bpy and RuL2-phen present an absorption around 491-495 nm, which is characteristic of most Ru(II) polypyridine complexes [86-89]. The MLCT band for $[Ru(tpy)_2]^{2+}$ in acetonitrile is observed around 474 nm. The shift to lower energy for other complexes where chloride is coordinated (500 nm) could be explained by destabilization of the metal $t_{2g}$ orbital which is caused by the chloride being a stronger $\pi$-donor than the pyridine ligand [86]. This same conclusion could be employed to explain the red shift of the charge transfer $d\pi(Ru(III))\rightarrow\pi^*(L)$-transitions in the Ru(II)-2(arylazo)pyridine derivatives, RuL1-(azpy, 3mazpy and tazpy) and RuL2--(azpy, 3mazpy and tazpy). The azo moiety is a better $\pi$-acid than bpy or phen and then the red shift of the metal-ligand charge transitions can be rationalized with the replacement of the azo functionality. The electronic spectra of $[Ru(tpy)(azpy)Cl]ClO_4$ has been recorded in acetonitrile and shows a similar pattern, with maximum absorptions at 680, 505, 325 and 310 nm [51].

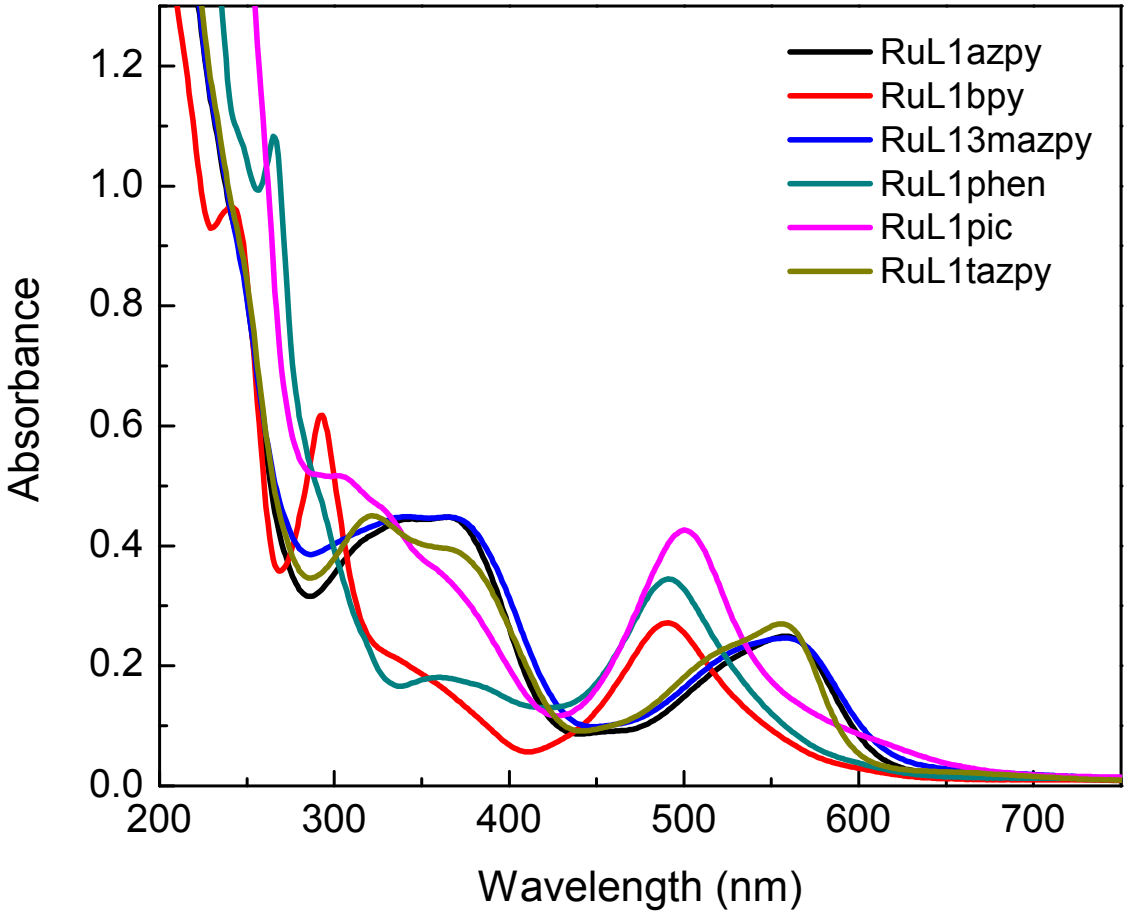


**Figure 5.7** Absorption spectra of Ru(II)L1-derivatives in acetonitrile at 294 K.

In the UV region the bands around 290 nm for RuL1-bpy and RuL2-bpy are assigned to bipyridine ligand $\pi\rightarrow\pi^*$-transitions and the bands around 265 nm are assigned to 1,10-phenanthroline ligand $\pi\rightarrow\pi^*$-charge transfer transitions. The same transitions are found in free bpy and phen at 263 and 279 nm, respectively which means that coordination of the ligands results in a red shift in the transition energy in the bpy system and a blue shift in the phen system [90].

The absorption spectra of RuL1-pic and RuL2-pic exhibit also a number of bands in the UV–Vis region. The spectral features in the visible region are attributed to the metal to ligand charge transitions which are comparable to the polypyridyl-Ru(II) charge transitions (figure 5.7) [73].

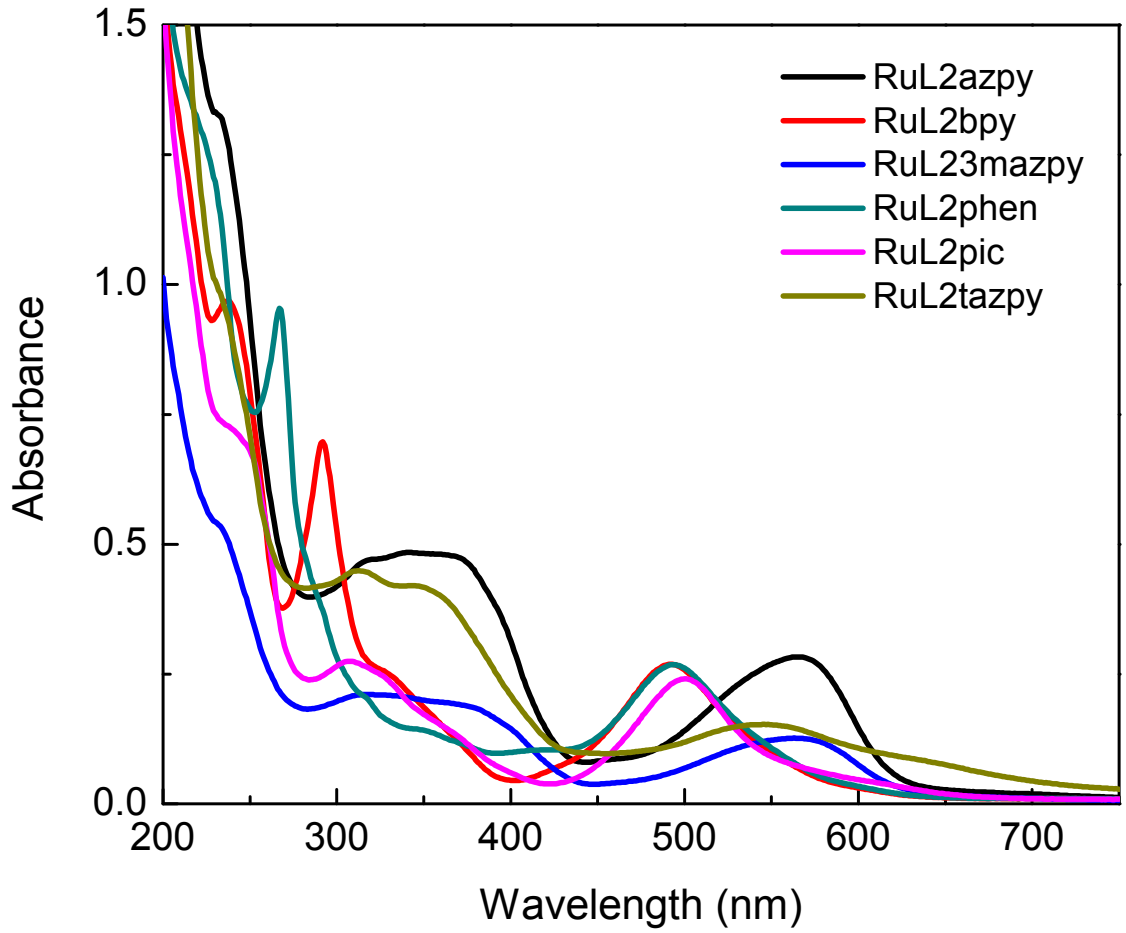


**Figure 5.8** Absorption spectra of Ru(II)L2-derivatives in acetonitrile at 294 K.

**E) NMR Spectroscopy.** As expected, the paramagnetic nature of the starting Ru(III) materials used is not observed in the products described in this chapter.

The $^{1}$H NMR spectra of Ru(II) compounds studied in this section, describe the diamagnetic nature of these Ru(II)-low spin complexes. The free ligands (azpy, bpy, 3mazpy, phen, pic and tazpy) and complexes display resolvable $^{1}$H NMR spectra in dmso, dmf, acetone, methanol and acetonitrile. They show all many sharp resonance peaks and all proton resonance signals were assigned by comparison with the starting materials and similar compounds (see chapter 3, RuL1-2(9EtGua)), integration values and confirmed by two dimensional COSY experiments, where separation of different groups of signals were achieved.

The spectra for some selected examples are described in figures 5.9, 5.10 and 5.11.

$^{1}$H NMR spectrum of RuL1-azpy (figure 5.9) in acetonitrile solution, shows thirteen sharp resonances, while in the structure are 36 protons.

In the tridentate ligand, due to the presence of a plane of symmetry, that goes through N1 and H3, the molecule can be split into two equal halves, and then the number of expected peaks is reduced by a half so 8 resonances are experimentally observed corresponding to the tridentate moiety. This evidence confirms the meridional coordination of the tridentate ligands L1. The integration of the signals corresponds to the 36 hydrogen atoms present in the complex.

In addition, the azpy moiety is clearly isolated from the group of resonances corresponding to the tridentate ligand and that is why the COSY experiments represent a useful tool for the characterization of these compounds (figure 5.10).

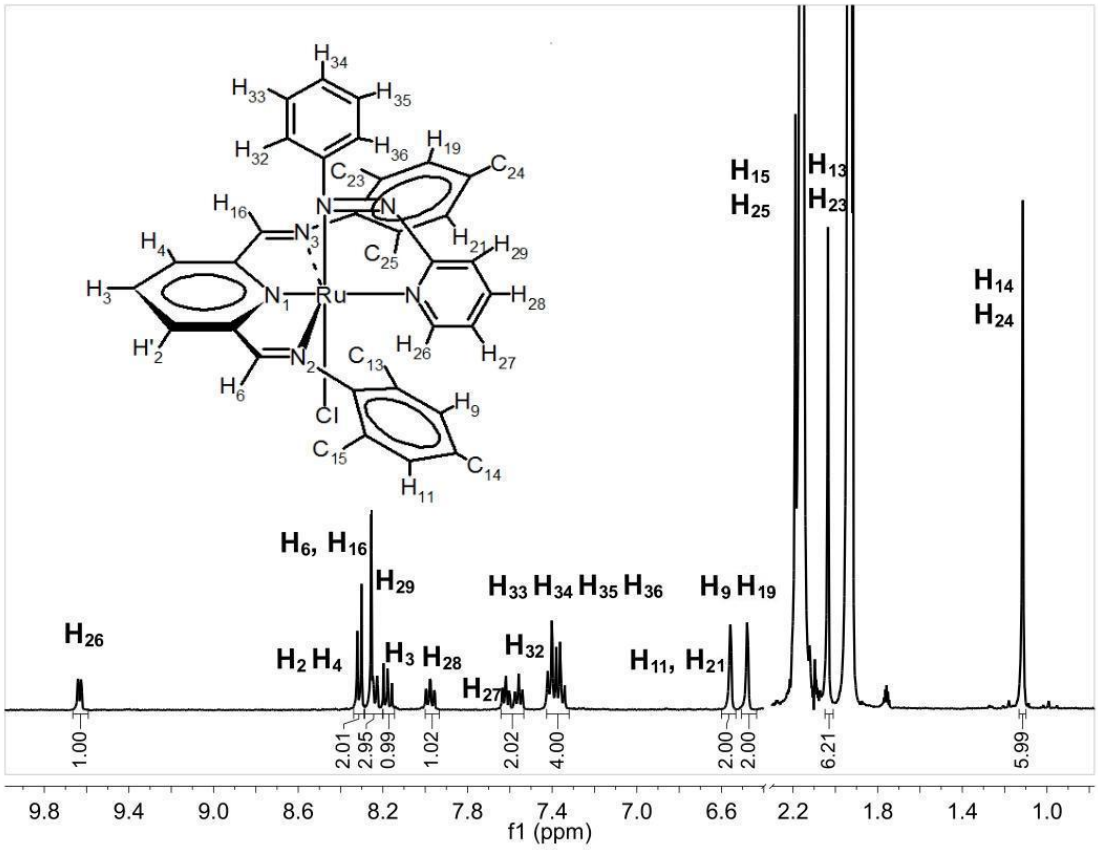


**Figure 5.9** $^{1}$H NMR spectrum of the RuL1-azpy, and corresponding assignment, recorded in deuterated acetonitrile (multiplet at 1.93 ppm) at 294 K. The numbering scheme proposed maintains consistency with numbering describe in the previous chapter. In the schematic representation, the hydrogen atoms belonging to the methyl groups have been omitted for clarity. A trace of water is visible at 2.16 ppm.

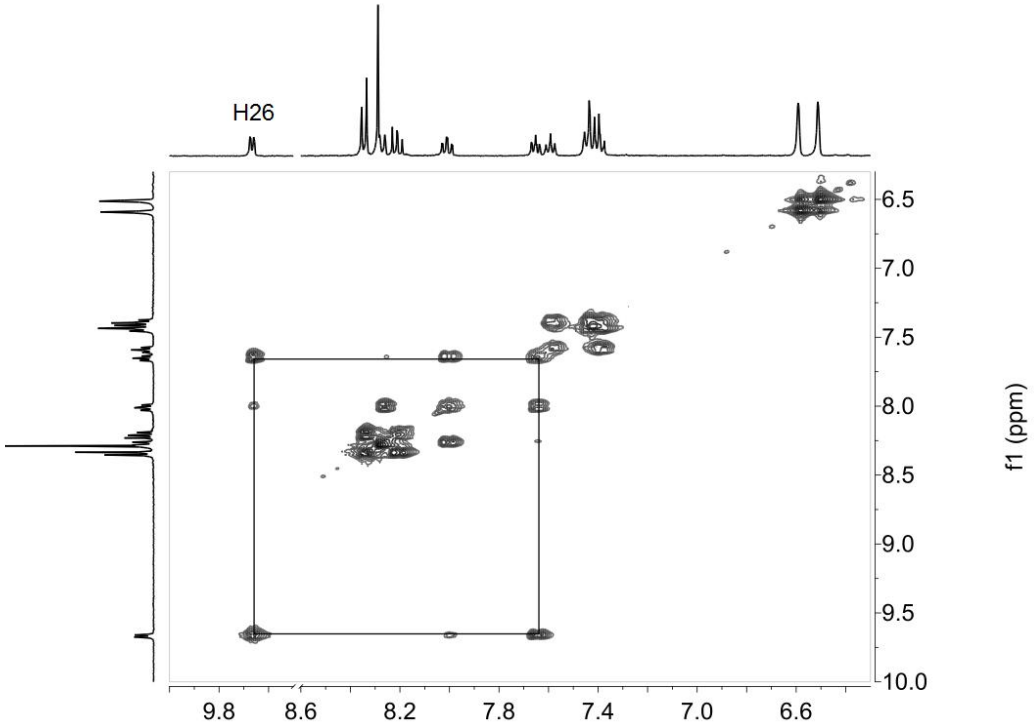


**Figure 5.10** 2D $^{1}$H COSY spectrum of RuL1-azpy recorded in deuterated acetonitrile at 294 K, using TMS as internal standard. Aromatic region is shown only.

Due to the asymmetric nature of azpy, 6 resonance peaks are experimentally observed. It is worth to mention that the intense deshielding effect observed in $H_{26}$ could be the result of coordination of azpy to the metal centre and also could be result of the close proximity with the

chloride ligand in the complex. In fact this evidence and the comparable reduced deshielding effect observed in $H_{28}$ clearly indicate that the coordination of the pyridine moiety of azpy in a *trans* arrangement with respect to the central pyridine in L1 is taking part. Same coordination modes have been reported in similar Ru(II)-azpy [91, 92] and $[Ru(tpy)(azpy)Cl]^+$ complexes [51, 63, 93]. If the coordination of the azpy-pyridine nitrogen would take part *trans* to the chloride ligand, the deshielding effect in $H_{28}$ would be stronger, producing a shift into values comparables to $H_{26}$ [36], partially due to the mesomeric effect in the ring. The paramagnetic influence of the pyridine ring of azpy is also clear, when the resonance peaks of hydrogen atoms $H_9$, $H_{11}$, $H_{19}$ and $H_{21}$ are analyzed. The upfield shift observed in these resonances must be generated by the spatially close paramagnetic currents from the pyridine ring of azpy. The very clean spectrum indicates a high purity of the sample and the absence of isomers. No relevant change in the spectrum was found after several days at 298 K.

Closely comparable results were obtained in case of RuL2-bpy, as observed in Figure 5.11, which shows the $^1$H NMR spectrum of RuL2-bpy and the corresponding peaks assignment. The hydrogen atom at *ortho* position in bpy ($H_{41}$), presents a deshielding effect which corresponds to coordination to the metal centre. This deshielding effect is also result of the close proximity of $H_{41}$ to the chloride atom in the complex. A similar effect has been reported for $[Ru(tpy)(bpy)Cl]^+$ and $[Ru(tpy)(phen)Cl]^+$ [93]. The protons in the pyridine ring of bpy (this is *trans* to the chloride atom), are affected differently. $H_{32}$ is not showing the same intense deshielding effect as $H_{41}$, most probably due to its magnetic environment, where paramagnetic currents from the pyridine ring in L2 are affecting its chemical shift.

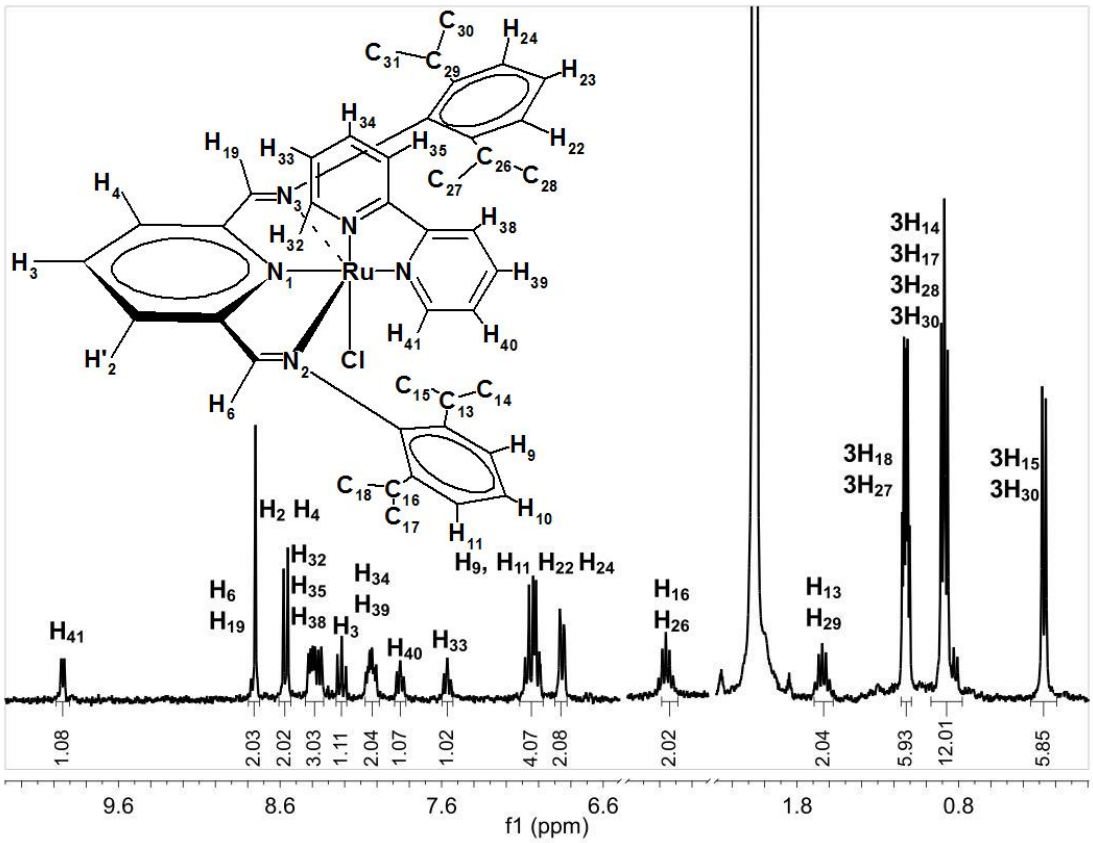


**Figure 5.11** $^1$H NMR spectrum of the RuL2-bpy, and corresponding assignment, recorded in deuterated acetonitrile (multiplet at 1.93 ppm) at 294 K. In the schematic representation, the hydrogen atoms belonging to the isopropyl groups have been omitted for clarity. The numbering scheme was selected in order to keep consistency with previous chapters.

The isopropyl moieties present different resonance peaks, due to differences in the magnetic environment. They are all doublets and their integration values are in agreement with the proposed structure. The hydrogen atoms in $C_{18}$ and $C_{27}$ must be in closer contact with the chloride atoms as higher deshielding effect is observed in the corresponding resonance peaks.

In table 5.5 and 5.6, a resume of the most relevant $^1$H NMR data, with the corresponding assignments, is presented. Because of the similar chemical environments in both families of

complexes it is not surprising to find out that the chemical shifts corresponding to protons in L1 or L2, ($H_2$, $H_3$, $H_4$, $H_6$, $H_{16}$ or $H_{19}$) are closely similar. Comparison of these values from both families of compounds, stress the fact that a small difference in the magnetic shifts is present. In general terms, more unprotected hydrogen atoms are observed for the family of RuL2 compounds. In fact, the chemical shift of equivalent $H_3$ hydrogen atoms in the central pyridine from tpy in the complexes, $[Ru(tpy)(bpy)Cl]^+$ and $[Ru(tpy)(phen)Cl]^+$ is 8.10 and 8.13 ppm, respectively [93], which are upfield shifted when compared with $H_3$ in RuL1-bpy, RuL2-bpy, RuL1-phen and RuL2-phen.

**Table 5.5** Selected $^1$H NMR data for the compounds RuL1-y; y=azpy, bpy, 3mazpy, phen, pic and tazpy. The aryl moieties from the tridentate L1, have been omitted for clarity reasons, while the bidentate ligand is represented by N~X . X could be the Nazo (azpy, 3mazpy and tazpy), Npy(bpy and phen) or O(pic) atoms.

| Compound | $^1$H NMR shift (ppm) Tridentate moiety | | | | Structure and numbering |
|---|---|---|---|---|---|
| | $H_6$, $H_{16}$ | $H_2$, $H_4$ | $H_3$ | *o*-Hpy(bidentate) | |
| RuL1-azpy | 8.26 | 8.31 | 8.18 | 9.63 trans N1 | 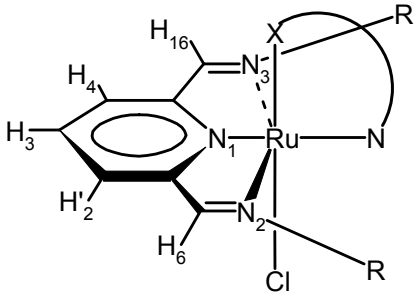 |
| RuL1-bpy | 8.67 | 8.46 | 8.22 | 9.91 trans N1 | |
| RuL1-3mazpy | 8.67 | 8.60 | 8.39 | 9.53 trans N1 | |
| RuL1-phen | 8.68 | 8.50 | 8.19 | 10.3 trans N1 | |
| RuL1-pic | 8.62 | 8.20 | 8.12 | 9.85 trans N1 | |
| RuL1-tazpy | 8.61 | 8.55 | 8.35 | 9.87 trans N1 | |



**Table 5.6** Selected $^1$H NMR data for the compounds RuL1-y ( y=azpy, bpy, 3mazpy, phen, pic and tazpy). The aryl moieties from the tridentate L2, have been omitted for clarity reasons while the bidentate ligand is represented by N~X . X could be the Nazo (azpy, 3mazpy and tazpy), Npy(bpy and phen) or O(pic) atoms.

| Compound | $^1$H NMR shift (ppm) Tridentate moiety | | | | Structure and numbering |
|---|---|---|---|---|---|
| | $H_6$, $H_{19}$ | $H_2$, $H_4$ | $H_3$ | o-Hpy(bidentate) | |
| RuL2-azpy | 8.79 | 8.76 | 8.53 | 9.51 trans N1 | 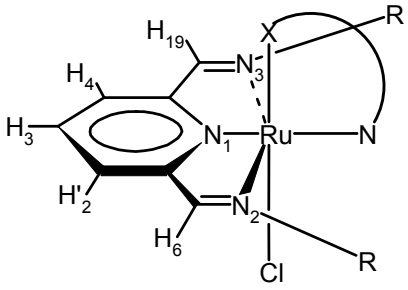 |
| RuL2-bpy | 8.72 | 8.56 | 8.22 | 9.94 trans N1 | |
| RuL2-3mazpy | 8.78 | 8.78 | 8.52 | 9.25 trans N1 | |
| RuL2-phen | 8.77 | 8.67 | 8.21 | 10.10 trans N1 | |
| RuL2-pic | 8.74 | 8.30 | 7.75 | 9.89 trans N1 | |
| RuL2-tazpy | 9.02 | 8.65 | 8.32 | 8.87 | |



Mayor differences are observed in the chemical shifts of the protons of the bidentate ligands. In particular, the changes in the resonance peaks of the hydrogen atoms from the bidentate ligands in *ortho* position (*o*-Hpy) of the nitrogen atom from the pyridine rings are of relevant value. In case of the RuL1 and RuL2 derivatives of bpy or phen, there is a dramatic downfield shift of one of the two hydrogen resonance peaks at *ortho* position of Npy ($H_{41}$ in RuL2-bpy, $H_{26}$ in RuL1-azpy, $H_{43}$ in RuL2-phen or $H_{26}$ in RuL1-pic, just for mentioning some), which has been explained as a consequence of coordination [93, 94]. For the compounds discussed in this chapter a major deshielding effect is observed for the *o*-Hpy resonance peaks in RuL1-phen and RuL2-phen (10.3 and 10.1 ppm, respectively). The chemical shift for the *o*-Hpy resonance peak of $[Ru(tpy)(phen)Cl]^+$ is 10.43 ppm [93]. In general terms, when comparing the chemical shifts of *o*-Hpy between both RuL1- and RuL2- families, slightly higher deshielding effects are observed for the RuL1-systems.

Some specific NMR properties for the RuL1 family of compounds should be mentioned. In case of RuL1-tazpy, the resonance peak that corresponds to the methyl substituent in the phenyl moiety displays an upfield shift (1.63 ppm) when comparing with the free tazpy (above 2.7 ppm, chapter 2, figures 2.1.2 and 2.3.4). This shift could just be explained with the azo group coordinated *trans* to Cl, so the paramagnetic currents in the pyridine ring of L1 are in close contact

with the methyl group generating this upfield shift. The $^1$H NMR spectrum of RuL1-3mazpy shows that similar arrangement in the structure must be taking part. A similar downfield shift for the o-Hpy proton signal RuL1-pic is observed, so the pyridine ring from 2-picolinate must be coordinated *trans* to the Npy in L1. This is further confirmed by the X-ray diffraction studies (figure 5.2).

In addition, some specific NMR data for the RuL2 family of compounds are discussed. It is clear from the chemical shift (*o*-Hpy) observed in all compound listed in table 5.6 that the pyridine ring from the bidentate ligand is coordinated *trans* to the pyridine ring in the tridentate ligand, as confirmed previously for the RuL1-family. RuL2-tazpy, by the contrary, presents an slightly different chemical shift. The previously observed upfield shift in the methyl resonance peak in RuL1-tazpy is not observed in the spectrum of RuL2-tazpy. The resonance peak is localized at 2.45 ppm, while in the free tazpy this peak is observed around 2.72 ppm. This evidence suggests that the arrangement is different. It is believed that the pyridine ring in tazpy is localized *trans* to the chloride ligand instead. This assumption is further supported by the observation of the *o*-Hpy peak around 8.87 ppm and the deshielding effect in $H_6$ and $H_{19}$ resonance peaks (table 5.5). This preferred coordination arrangement must probably be directed by strong steric repulsions within the coordination sphere, generated by the isopropyl groups.

### 5.3.2 Cytotoxic activity studies

The experimental details in the determination of the cytotoxicity activity of the compounds studied were fully described in the experimental section and the $IC_{50}$ values were evaluated in seven human cell lines, i.e. A498, EVSA-T, H226, IGROV, M19, MCF-7 and WIDR. Cisplatin and doxorubicin were used as reference cytotoxic compounds. The $IC_{50}$ values that were obtained after continuous exposure of the cells to the compounds for 120 h are concentrated in table 5.7. The $IC_{50}$ value represents the minimal amount of drug needed to inhibit 50% of the cancer cell growth.

**Table 5.7** *In vitro* cytotoxicity assay of compounds synthesized incubated during 120 h.

| Compound | Cell line[a], $IC_{50}$ (μM) | | | | | | |
|---|---|---|---|---|---|---|---|
| | A498 | EVSA-T | H226 | IGROV | M19 | MCF-7 | WIDR |
| RuL1 | 15.1 | 11.2 | 15.2 | 12.2 | 12.2 | 17.1 | 14.5 |
| RuL2 | 4.1 | 4.0 | 4.3 | 4.1 | 3.9 | 4.3 | 4.1 |
| $[Ru(tpy)Cl_3]$ | 79.6 | 67.0 | 63.7 | 90.1 | 68.5 | 64.0 | 79.0 |
| $[Ru(tpy)(azpy)Cl]Cl5H_2O$[b] | 39.3 | 11.4 | 33.6 | 64.8 | 14.6 | 30.5 | 51.0 |
| RuL1-azpy | 4.1 | 0.5 | 3.0 | 6.5 | 0.6 | 1.7 | 2.2 |
| RuL1-bpy | 19.2 | 0.8 | 9.1 | 3.7 | 1.5 | 2.2 | 3.1 |
| **RuL1-3mazpy** | **2.9** | **0.4** | **1.8** | **2.0** | **0.4** | **0.8** | **1.4** |
| RuL1-phen | 9.7 | 0.4 | 3.6 | 1.9 | 1.0 | 1.0 | 1.5 |
| RuL1-pic | 18.0 | 1.4 | 13.4 | 26.7 | 2.0 | 4.2 | 10.5 |
| RuL1-tazpy | 5.7 | 0.6 | 3.2 | 2.8 | 0.9 | 1.5 | 2.3 |
| RuL2-azpy | 6.0 | 1.2 | 3.2 | 2.9 | 1.3 | 1.5 | 1.9 |
| RuL2-bpy | 4.0 | 1.1 | 1.5 | 1.4 | 1.3 | 1.2 | 1.3 |
| **RuL2-3mazpy** | **1.6** | **0.4** | **1.2** | **1.5** | **0.5** | **0.6** | **0.9** |
| **RuL2-phen** | **1.4** | **1.0** | **1.3** | **1.8** | **1.3** | **1.2** | **1.3** |
| RuL2-pic | 5.8 | 1.8 | 5.5 | 10.6 | 5.2 | 3.3 | 4.0 |
| **RuL2-tazpy** | **1.4** | **0.5** | **1.0** | **1.1** | **0.7** | **0.6** | **0.9** |
| $\alpha$-$[Ru(azpy)_2Cl_2]$[c] | 0.3 | 0.06 | 0.5 | 0.3 | 0.06 | 0.3 | 0.3 |
| Cisplatin | 7.5 | 1.4 | 10.9 | 0.6 | 1.9 | 2.3 | 3.2 |
| DOX | 0.16 | 0.015 | 0.37 | 0.11 | 0.03 | 0.02 | 0.02 |

[a] A498 Human renal carcinoma cell line; EVSA-T Human breast cancer cell line; H226 Human non-small cell lung carcinoma cell line; IGROV Human ovarian carcinoma cell line; M19 Human melanoma carcinoma cell line; MCF-7 Human breast adenocarcinoma cell line; WIDR Human colon adenocarcinoma cell line.[b] [55]. [c] [36]

From the above results, it appears that the family of RuL2-compounds present better cytotoxic values. However, the starting material Ru(III)L2, also shows better cytotoxic values when compared with RuL1, and some of the RuL1-derivatives show promising values as well. This evidence suggest that the structure activity relationship is even more complicated. It is important to stress the fact that most of the compounds tested present better cytotoxic activity than cisplatin and even comparable values with $\alpha$-$[Ru(azpy)_2Cl_2]$, the most potent cytotoxic Ru(II) agent described in literature [10, 12, 36, 91]. The presence of their cytotoxic activity by itself probes that all tested compounds are able to travel inside the cells.

It is observed in general terms that the $IC_{50}$ values are reduced by one third when reducing the oxidation state of the metal centre and interestingly low values are observed in the cell lines EVSA-T, M19 and MCF-7, which are also particularly sensitive to the presence of $\alpha$-$[Ru(azpy)_2Cl_2]$. Almost the same selectivity has been observed in the starting Ru(III)-materials RuL1 and RuL2 (EVSA-T, IGROV and M19). The small structural difference between the RuL2- and RuL1-families of compounds, where the RuL2-series contains a more bulky ligand (L2), is sufficient for the 3-fold increase in the cytotoxic activity. Although a discussion about the mechanism of activity is still premature, it is clear, that the biological activity is affected by both electronic and steric factors. It can be proposed that the steric effects can reduce the rate of hydrolysis or other substitution reactions in the RuL2-series of compound and, at the same time, the ligand, a bis(arylimino)pyridine derivative, with the imino moieties (known to have better $\pi$-backbonding properties than pyridine) can stabilize more efficiently lower oxidation states of the metal centre.

For both families of compounds, the coordination of 3mazpy produces the better cytotoxic values while the coordination of pic induces the lower $IC_{50}$ values. Certainly, the reduction in the basicity of the bidentate ligands (qualitative basicity: phen>bpy>3mazpy>azpy~tazpy>pic) has a negative influence in the cytotoxic effect ($IC_{50}^{RuL1\text{-}3mazpy} > IC_{50}^{RuL1\text{-}pic}$), but it is not the only factor taking part as RuL1- and RuL2-phen or RuL1- and RuL2-bpy have a smaller biological effect than the 3mazpy derivatives. Among the 2-(phenylazo)pyridine derivatives the higher the basicity, the better the $IC_{50}$ values with the only exception of RuL2-tazpy. This discrepancy could be associated to the different spatial organization presented in this compound, previously discussed (NMR spectroscopy section). As suggested by $\alpha$-$[Ru(azpy)_2Cl_2]$, the flexibility in the azpy ligand could have an important effect in the cytotoxic activity and this could be also related to the previous results.

Due to the close structural similarities between RuL1, RuL2 and $[Ru(tpy)Cl_3]$, the cytotoxic effect of $[Ru(tpy)(azpy)Cl]^+$ was evaluated for comparison reasons. RuL1-azpy and RuL2-azpy show around 10-times better cytotoxic effects than $[Ru(tpy)(azpy)Cl]^+$ with the best values reported for RuL1-azpy.

The reasons behind the differences in the cytotoxic activities just discussed are far from understood, and clearly more studies with different cell lines and *in vitro* studies with biologically relevant structures, like proteins, DNA and reducing agents, and determination of redox properties, are required. Also structural modifications that improve even more the solubility properties will be of help.

In summary, from the results presented by these families of Ru compounds, the compounds present promising anticancer activity, some of them even with tissue-selective cytotoxic properties and this may warrant further investigation as anticancer drug leads in the field of Ru anticancer compounds.

## 5.4 Conclusions

The success in the synthesis of highly cytotoxic active Ru(III)-bis(arylimino)pyridine derivatives has urged the development of other Ru(II) derivatives in search of even more potent anticancer drug candidates. Then a series of mononuclear ruthenium complexes of the type $[Ru(Lx)(Ly)Cl]^+$ (Lx=L1: 2,6-bis(2,4,6-trimethylphenyliminomethyl)pyridine or L2: 2,6-bis(2,6-diisopropylphenyliminomethyl) pyridine and Ly= azpy, bpy, 3mazpy, phen, pic and tazpy) were prepared, isolated and characterized by elemental analysis, IR, $^1$H-NMR, ESI-MS, UV-Vis and in some cases by X-ray diffraction studies.

The synthesis of the Ru(II) complexes with several bidentate ligands has been achieved by a single step procedure in moderate-to-high yields.

The complexes, incorporating bidentate ligands with different donor atoms nature, are also designed to contain a monodentate chloride ligand, which would be easily substituted.

This research has led the development of a promising new generation of potential antineoplastic Ru(II) compounds with bis(arylimino)pyridine ligands. The potential interest lies mainly in the facility of modifications of the tridentate ligand moiety, which could help in the tuning of the biological properties with special interest in maximizing the cytotoxic activity, but also represent plausible active catalytic compounds in the field of metal-bis(imino)pyridine systems that have attracted significant attention in recent years.

The *in vitro* cytotoxic effect of these complexes in several tumor cell lines was also studied. They present moderate to high cytotoxic effect and some of them show even better cytotoxic activity than cisplatin and are comparable to the cytotoxic activity of $\alpha$-[Ru(azpy)$_2$Cl$_2$]. The i*n vitro* evaluation of the cytotoxic properties of these new Ru(II) complexes in comparison with the parent Ru(III)-compounds ($IC_{50}$ values = 4 ~ 17 $\mu$M) led to significant improvement in cytotoxicity ($IC_{50}$ values =0.4 ~ 10 $\mu$M) for a broad range of cancer cell-lines tested. Complexes RuL1-3mazpy and RuL2-3mazpy have produced the better $IC_{50}$ values. Overall, the $IC_{50}$ values for the RuL2-family of compounds are lowest, although some RuL1-derivatives also show remarkably high cytotoxic effect.

The potent cytotoxic activity observed for these family of Ru(II)-bis(arylimino)pyridine compounds stresses the need for more studies comprising the *in vitro* cytotoxic activity determination in different cell lines, the interaction with biologically relevant structures, like proteins, DNA, nucleotides and reducing agents (ascorbic acid, cysteine or glutathione), and the redox and aquation/hydrolysis properties as well. Also structural modifications that improve the solubility properties are recommended.

## 5.5 References


[1] J. Mola, I. Romero, M. Rodriguez, F. Bozoglian, A. Poater, M. Sola, T. Parella, J. Benet-Buchholz, X. Fontrodona, A. Llobet, Inorg. Chem. 46 (2007) 10707-10716.

[2] J. Reedijk, Platinum Metals Rev. 52 (2008) 2-11.

[3] A. Gerli, J. Reedijk, M.T. Lakin, A.L. Spek, Inorg. Chem. 34 (1995) 1836-1843.

[4] A. Llobet, P. Doppelt, T.J. Meyer, Inorg. Chem. 27 (1988) 514-520.

[5] P.K. Sinha, J. Chakravarty, S. Bhattacharya, Polyhedron 15 (1996) 2931-2938.

[6] W.Y. Yu, W.C. Cheng, C.M. Che, Y. Wang, Polyhedron 13 (1994) 2963-2969.

[7] O. Novakova, J. Kasparkova, O. Vrana, P.M. van Vliet, J. Reedijk, V. Brabec, Biochemistry 34 (1995) 12369-12378.

[8] P.M. van Vliet, S.M.S. Toekimin, J.G. Haasnoot, J. Reedijk, O. Novakova, O. Vrana, V. Brabec, Inorg. Chim. Acta 231 (1995) 57-64.

[9] M.J. Clarke, F.C. Zhu, D.R. Frasca, Chem. Rev. 99 (1999) 2511-2533.

[10] A.C.G. Hotze, A.H. Velders, F. Ugozzoli, M. Biagini-Cingi, A.M. Manotti-Lanfredi, J.G. Haasnoot, J. Reedijk, Inorg. Chem. 39 (2000) 3838-3844.

[11] A.H. Velders, K. van der Schilden, A.C.G. Hotze, J. Reedijk, H. Kooijman, A.L. Spek, Dalton Trans. (2004) 448-455.

[12] A.C.G. Hotze, M. Bacac, A.H. Velders, B.A.J. Jansen, H. Kooijman, A.L. Spek, J.G. Haasnoot, J. Reedijk, J. Med. Chem. 46 (2003) 1743-1750.

[13] L. Ronconi, P.J. Sadler, Coord. Chem. Rev. 251 (2007) 1633-1648.

[14] M. Melchart, A. Habtemariam, S. Parsons, P.J. Sadler, J. Inorg. Biochem. 101 (2007) 1903-1912.

[15] R.E. Morris, R.E. Aird, P.D. Murdoch, H.M. Chen, J. Cummings, N.D. Hughes, S. Parsons, A. Parkin, G. Boyd, D.I. Jodrell, P.J. Sadler, J. Med. Chem. 44 (2001) 3616-3621.

[16] R.E. Aird, J. Cummings, A.A. Ritchie, M. Muir, R.E. Morris, H. Chen, P.J. Sadler, D.I. Jodrell, Br. J. Cancer 86 (2002) 1652-1657.

[17] C.G. Hartinger, S. Zorbas-Seifried, M.A. Jakupec, B. Kynast, H. Zorbas, B.K. Keppler, J. Inorg. Biochem. 100 (2006) 891-904.

[18] I. Kostova, Curr. Med. Chem. 13 (2006) 1085-1107.

[19] E. Reisner, V.B. Arion, B.K. Keppler, A.J.L. Pombeiro, Inorg. Chim. Acta 361 (2008) 1569-1583.

[20] R.A. Vilaplana, F. Gonzalezvilchez, E. Gutierrezpuebla, C. Ruizvalero, Inorg. Chim. Acta 224 (1994) 15-18.

[21] R. Vilaplana, Metal-Based Drugs. 2 (1995) 211-219.

[22] F. Gonzalez-Vilchez, R. Vilaplana, G. Blasco, L. Messori, J. Inorg. Biochem. 71 (1998) 45-51.

[23] G. Sava, S. Pacor, A. Bergamo, M. Cocchietto, G. Mestroni, E. Alessio, Chem.-Biol. Interact. 95 (1995) 109-126.

[24] G. Sava, F. Frausin, M. Cocchietto, F. Vita, E. Podda, P. Spessotto, A. Furlani, V. Scarcia, G. Zabucchi, Eur. J. Cancer 40 (2004) 1383-1396.
[25] W.H. Ang, E. Daldini, C. Scolaro, R. Scopelliti, L. Juillerat-Jeannerat, P.J. Dyson, Inorg. Chem. 45 (2006) 9006-9013.
[26] W.H. Ang, P.J. Dyson, Eur. J. Inorg. Chem. (2006) 4003-4018.
[27] P.J. Dyson, G. Sava, Dalton Trans. (2006) 1929-1933.
[28] M.J. Clarke, Coord. Chem. Rev. 236 (2003) 209-233.
[29] F. Kratz, M. Hartmann, B. Keppler, L. Messori, J. Biol. Chem. 269 (1994) 2581-2588.
[30] F. Kratz, L. Messori, J. Inorg. Biochem. 49 (1993) 79-82.
[31] P. Som, Z.H. Oster, K. Matsui, G. Guglielmi, B.R.R. Persson, M.L. Pellettieri, S.C. Srivastava, P. Richards, H.L. Atkins, A.B. Brill, Eur. J. Nucl. Med. 8 (1983) 491-494.
[32] H.Z. Sun, H.Y. Li, P.J. Sadler, Chem. Rev. 99 (1999) 2817-2842.
[33] L. Messori, F. Kratz, E. Alessio, Met.-Based Drugs 3 (1996) 1-9.
[34] F. Kratz, B.K. Keppler, L. Messori, C. Smith, E.N. Baker, Met.-Based Drugs 1 (1994) 169-173.
[35] J.G. Vos, J.M. Kelly, Dalton Trans. (2006) 4869-4883.
[36] A.C.G. Hotze, 'Design of ruthenium anticancer agents. Study of the structure-activity relationships and binding to DNA model bases of ruthenium complexes with 2-phenylazopyridine ligands', PhD Thesis, Leiden University, Leiden, 2003.
[37] K.N. Mitra, S. Choudhury, S. Goswami, S.M. Peng, Polyhedron 16 (1997) 1605-1614.
[38] Nonius, COLLECT; Nonius BV, Delft: The Netherlands (1999).
[39] A.M.M. Schreurs, PEAKREF, University of Utrecht:The Netherlands (2005).
[40] A.J.M. Duisenberg, L.M.J. Kroon-Batenburg, A.M.M. Schreurs, J. Appl. Cryst. 36 (2003) 220-229.
[41] P.T. Beurskens, G. Beurskens, R. de Gelder, S. Garcia-Granda, R.O. Gould, R. Israel, J.M.M. Smits, The DIRDIF99 Program System, Technical Report of the Crystallography Laboratory; University of Nijmegen: The Netherlands (1999).
[42] G.M. Sheldrick, Acta Cryst. A64 (2008) 112-122.
[43] G.M. Sheldrick, SADABS; University of Göttingen: Germany (1999-2003).
[44] A.L. Spek, J. Appl. Crystallogr. 36 (2003) 7-13.
[45] Y.P. Keepers, P.E. Pizao, G.J. Peters, J. Vanarkotte, B. Winograd, H.M. Pinedo, Eur. J. Cancer 27 (1991) 897-900.
[46] M.R. Boyd, in 'Status of the NCI preclinical antitumour drug discovery screen ', ed. NCI, Principles and practice of oncology, 1989, 1-12.
[47] T.S.B. Baul, C. Masharing, G. Ruisi, R. Jirasko, M. Holcapek, D. de Vos, D. Wolstenholme, A. Linden, J. Organomet. Chem. 692 (2007) 4849-4862.
[48] D. Chatterjee, A. Sengupta, A. Mitra, Polyhedron 26 (2007) 178-183.
[49] K.J. Takeuchi, M.S. Thompson, D.W. Pipes, T.J. Meyer, Inorg. Chem. 23 (1984) 1845-1851.
[50] N. Chanda, S.M. Mobin, V.G. Puranik, A. Datta, M. Niemeyer, G.K. Lahiri, Inorg. Chem. 43 (2004) 1056-1064.
[51] N.C. Pramanik, K. Pramanik, P. Ghosh, S. Bhattacharya, Polyhedron 17 (1998) 1525-1534.
[52] S. Sarkar, B. Sarkar, N. Chanda, S. Kar, S.M. Mobin, J. Fiedler, W. Kaim, G.K. Lahiri, Inorg. Chem. 44 (2005) 6092-6099.
[53] B.J. Coe, D.W. Thompson, C.T. Culbertson, J.R. Schoonover, T.J. Meyer, Inorg. Chem. 34 (1995) 3385-3395.
[54] X.J. Yang, F. Drepper, B. Wu, W.H. Sun, W. Haehnel, C. Janiak, Dalton Trans. (2005) 256-267.
[55] E. Corral, A.C.G. Hotze, T. D.M., A.L. Spek, J. Reedijk, Inorg. Chim. Acta 359 (2006) 830-838.
[56] S. Patra, B. Sarkar, S. Ghumaan, M.P. Patil, S.M. Mobin, R.B. Sunoj, W. Kaim, G.K. Lahiri, Dalton Trans. (2005) 1188-1194.
[57] N.C. Pramanik, S. Bhattacharya, Transit. Met. Chem. 22 (1997) 524-526.
[58] S. Goswami, A.R. Chakravarty, A. Chakravorty, Inorg. Chem. 20 (1981) 2246-2250.
[59] R.A. Krause, K. Krause, Inorg. Chem. 19 (1980) 2600-2603.
[60] N.C. Pramanik, S. Bhattacharya, Polyhedron 16 (1997) 1755-1761.
[61] G.K. Lahiri, S. Bhattacharya, M. Mukherjee, A.K. Mukherjee, A. Chakravorty, Inorg. Chem. 26 (1987) 3359-3365.
[62] B. Cetinkaya, E. Cetinkaya, M. Brookhart, P.S. White, J. Mol. Catal. A-Chem. 142 (1999) 101-112.
[63] B. Mondal, M.G. Walawalkar, G.K. Lahiri, J. Chem. Soc.-Dalton Trans. (2000) 4209-4217.
[64] A.L. Spek, A. Gerli, J. Reedijk, Acta Crystallogr. Sect. C-Cryst. Struct. Commun. 50 (1994) 394-397.
[65] G.J.P. Britovsek, M. Bruce, V.C. Gibson, B.S. Kimberley, P.J. Maddox, S. Mastroianni, S.J. McTavish, C. Redshaw, G.A. Solan, S. Stromberg, A.J.P. White, D.J. Williams, J. Am. Chem. Soc. 121 (1999) 8728-8740.
[66] B. Mondal, S. Chakraborty, P. Munshi, M.G. Walawalkar, G.K. Lahiri, J. Chem. Soc.-Dalton Trans. (2000) 2327-2335.
[67] E.L. Dias, M. Brookhart, P.S. White, Organometallics 19 (2000) 4995-5004.
[68] S. Pal, S. Pal, Polyhedron 22 (2003) 867-873.
[69] S.N. Pal, S. Pal, Acta Crystallogr. C 58 (2002) m273-m275.
[70] A.E.M. Boelrijk, J. Reedijk, J. Mol. Catal. A-Chem. 89 (1994) 63-75.
[71] S. Pal, S. Pal, Z. Anorg. Allg. Chem. 628 (2002) 2091-2098.
[72] S. Fukui, Y. Shimamura, Y. Sunamoto, T. Abe, T. Hirano, T. Oi, H. Nagao, Polyhedron 26 (2007) 4645-4652.
[73] A.A. Rachford, J.L. Petersen, J.J. Rack, Dalton Trans. (2007) 3245–3251.
[74] A. Benaltabef, S.B.R. Degallo, M.E. Folquer, N.E. Katz, Inorg. Chim. Acta 188 (1991) 67-70.
[75] C.R. Hecker, P.E. Fanwick, D.R. McMillin, Inorg. Chem. 30 (1991) 659-666.
[76] N.E. Holden, CRC Press. Boca Raton, Florida CRC Handbook of Chemistry and Physics, David R. Lide (ed.), 85th Edition, (2005).

[77] T.D. Thangadurai, S.K. Ihm, Transit. Met. Chem. 29 (2004) 189-195.
[78] S. Pal, S. Pal, J. Chem. Soc.-Dalton Trans. (2002) 2102-2108.
[79] S. Youngme, G.A. van Albada, N. Chaichit, P. Gunnasoot, P. Kongsaeree, I. Mutikainen, O. Roubeau, J. Reedijk, U. Turpeinen, Inorg. Chim. Acta 353 (2003) 119-128.
[80] S. Pal, C. Sinha, Transit. Met. Chem. 27 (2002) 218-222.
[81] N. Ghatak, J. Chakravarty, S. Bhattacharya, Transit. Met. Chem. 20 (1995) 138-141.
[82] N. Ghatak, J. Chakravarty, S. Bhattacharya, Polyhedron 14 (1995) 3591-3597.
[83] X. Sala, N. Santana, I. Serrano, E. Plantalech, I. Romero, M. Rodriguez, A. Llobet, S. Jansat, M. Gomez, X. Fontrodona, Eur. J. Inorg. Chem. (2007) 5207-5214.
[84] S.C. Rasmussen, S.E. Ronco, D.A. Mlsna, M.A. Billadeau, W.T. Pennington, J.W. Kolis, J.D. Petersen, Inorg. Chem. 34 (1995) 821-829.
[85] P.A. Anderson, G.B. Deacon, K.H. Haarmann, F.R. Keene, T.J. Meyer, D.A. Reitsma, B.W. Skelton, G.F. Strouse, N.C. Thomas, J.A. Treadway, A.H. White, Inorg. Chem. 34 (1995) 6145-6157.
[86] C. Bonnefous, A. Chouai, R.P. Thummel, Inorg. Chem. 40 (2001) 5851-5859.
[87] A. Juris, V. Balzani, F. Barigelletti, S. Campagna, P. Belser, A. Vonzelewsky, Coord. Chem. Rev. 84 (1988) 85-277.
[88] V.G. Vaidyanathan, B.U. Nair, Dalton Trans. (2005) 2842-2848.
[89] A. Anthonysamy, S. Balasubramanian, V. Shanmugaiah, N. Mathivanan, Dalton Trans. (2008) 2136-2143.
[90] U.K. Mazumder, M. Gupta, S.S. Karki, S. Bhattacharya, S. Rathinasamy, S. Thangavel, Chem. Pharm. Bull. 52 (2004) 178-185.
[91] A.C.G. Hotze, S.E. Caspers, D. de Vos, H. Kooijman, A.L. Spek, A. Flamigni, M. Bacac, G. Sava, J.G. Haasnoot, J. Reedijk, J. Biol. Inorg. Chem. 9 (2004) 354-364.
[92] A.C.G. Hotze, E.P.L. van der Geer, H. Kooijman, A.L. Spek, J.G. Haasnoot, J. Reedijk, Eur. J. Inorg. Chem. (2005) 2648-2657.
[93] W.K. Seok, S.W. Moon, M.Y. Kim, Bull. Korean Chem. Soc. 19 (1998) 1207-1211.
[94] E.C. Constable, M.J. Hannon, Inorg. Chim. Acta 211 (1993) 101-110.